PHYSICAL REVIEW B VOLUME 16, NUMBER 3 1 AUGUST 1977

Renormalization, vortices, and symmetry-breaking perturbations in the two-dimensional planar model

Jorge V. José*† and Leo P. Kadanoff*
Department of Physics, Brown University, Providence, Rhode Island 02912

Scott Kirkpatrick
Department of Physics, State University of New York at Stony Brook, Stony Brook, New York 11794 and IBM Thomas J. Watson Research Center,‡ Yorktown Heights, New York 10598

David R. Nelson§
Department of Physics, Harvard University, Cambridge, Massachusetts 12138
(Received 7 March 1977)

The classical planar Heisenberg model is studied at low temperatures by means of renormalization theory and a series of exact transformations. A numerical study of the Migdal recursion relation suggests that models with short-range isotropic interactions rapidly become equivalent to a simplified model system proposed by Villain. A series of exact transformations then allows us to treat the Villain model analytically at low temperatures. To lowest order in a parameter which becomes exponentially small with decreasing temperature, we reproduce results obtained previously by Kosterlitz. We also examine the effect of symmetry-breaking crystalline fields on the isotropic planar model. A numerical study of the Migdal recursion scheme suggests that these fields (which must occur in real quasi-two-dimensional crystals) are strongly *relevant* variables, leading to critical behavior distinct from that found for the planar model. However, a more exact low-temperature treatment of the Villain model shows that *hexagonal* crystalline fields eventually become irrelevant at temperatures below the T_c of the isotropic model. Isotropic planar critical behavior should be experimentally accessible in this case. *Nonuniversal* behavior may result if cubic crystalline fields dominate the symmetry breaking. Interesting duality transformations, which aid in the analysis of symmetry-breaking fields are also discussed.

I. INTRODUCTION

A. Planar model

We wish to examine the low-temperature properties of the classical planar Heisenberg model of ferromagnetism in two dimensions. Thus, we consider a reduced Hamiltonian or "action" of the form

$$A[\theta] \equiv \frac{-H}{k_B T} = -\sum_{\langle \vec{r}, \vec{r}' \rangle} K\{1 - \cos[\theta(\vec{r}) - \theta(\vec{r}')]\} + \sum_{\vec{r}} \sum_{p} h_p \cos[p\theta(\vec{r})], \tag{1.1}$$

where the sums over $\vec{r}$ index the sites of a two-dimensional lattice, the symbol $\langle \vec{r}, \vec{r}' \rangle$ indicates a sum over nearest-neighbor lattice sites only, and

$$K = J/k_B T. \tag{1.2}$$

The quantity J is an exchange coupling entering a nearest-neighbor interaction between fixed length spins on the lattice of the form $J\vec{S}(\vec{r})\cdot\vec{S}(\vec{r}')$, and $\theta(\vec{r})$ is the angle the spin $\vec{S}(\vec{r})$ makes with some arbitrary axis. The second term in (1.1) involves a sum over possible symmetry-breaking fields h_p indexed by a positive integer p.

With all symmetry-breaking fields h_p set to zero, the Hamiltonian (1.1) has been studied quite extensively. Although evidence from high-temperature series expansions[1-3] suggests that the susceptibility of the planar model diverges at some finite T_c, the lack of long-range order at any temperature has been proven rigorously.[4-6]

Wegner[7] and Berezinskii,[8] and later Zittartz,[9] have produced "spin wave" theories for the planar model which should be accurate at sufficiently low temperatures. This class of theories leads to a power-law decay of correlation functions at all temperatures, suggesting that the model has a line of critical points with continuously variable critical exponents. Taken literally, the spin-wave results suggest that this line extends out to infinite temperature.

Kosterlitz and Thouless[10] and Berezinskii[11] suggested that the spin-wave theories should be modified in an important way by the presence of vortex excitations in the model. Below a certain critical temperature, bound vortex-antivortex pairs should populate an "ordered phase," coexisting with the spin-wave excitations. Above T_c, these pairs are expected to dissociate. Kosterlitz[12] subsequently produced a quantitative analysis

which makes this picture concrete. He constructed a simple renormalization-group transformation which contains a line of fixed points, corresponding physically to a line of critical points terminating in a finite $T_c < \infty$.[13]

In this paper, we focus especially upon the region $T < T_c$. Two methods of attack are developed here. First, the planar model is examined directly via a lattice recursion scheme introduced by Migdal.[14] When applied to fixed-length spins in $2+\epsilon$ dimensions, this scheme is known to yield results equivalent to those obtained in a more sophisticated theory[15,16] to first order in ϵ. Second, we argue that there is another model—a generalized Villain[17,18] model—which has exactly the same symmetry properties as the planar model but is easier to analyze. The original Villain model makes the Kosterlitz-Thouless decomposition into spin waves and vortices particularly simple because the spin waves are described by a purely Gaussian (and hence soluble) interaction. Our generalized Villain model includes (in addition to the coupling strength K) a parameter y which determines the strength of the coupling of vortices into the spin-wave system. In the low-temperature region, one can gain very useful results by expanding in the additional parameter y.

Our plan of attack will be to use the Migdal approximation to understand in a semiquantitative fashion the planar model's behavior. We will argue that this approximation gives recursion relations which become more and more quantitively correct as the temperature goes to zero. Unfortunately, some of the apparent qualitative features of the exact problem—in particular the existence of a fixed line—are not correctly given by the Migdal scheme. But, the fixed line is almost[19] present so that one can gain useful insight from this approach.

Then, armed with this insight, we pass from the Midgal approximation to the generalized Villain model. This interaction will very naturally lead to a perturbation scheme. This scheme will be very similar to the Kosterlitz-Thouless decomposition into spin waves and vortices, followed by an expansion in the vortex variables. We shall argue that this expansion converges for all temperatures lower than the Kosterlitz-Thouless transition temperature T_c at which the vortices can become unbound.

From the theoretical point of view, our major result will be that the Gaussian spin-wave theory is quantitively exact for predicting the large-distance correlation functions of the planar model at any temperature below T_c. In particular the correlation function for $\cos p\theta(r)$ is given by the spin-wave result

$$\langle \cos p\theta(r) \cos p\theta(r') \rangle \sim (|r - r'|^{p^2/2\pi K_{\text{eff}}})^{-1} \quad (1.3)$$

for all values of p equal to integers. This result, we argue, is true for large $|\vec{r} - \vec{r}'|$ for all the models in question whenever the symmetry-breaking terms [defined by h_p in Eq. (1.1)] are zero. The models differ in that K_{eff} depends differently upon K for the various cases. But in all cases $K_{\text{eff}} \to K$, as $K \to \infty (T \to 0)$. As the temperature increases, K decreases and so does K_{eff}—albeit in a model-dependent fashion. This decrement in K_{eff} continues until

$$2\pi K_{\text{eff}} = 4 , \quad (1.4)$$

whereupon we observe an unbinding of the vortices and a transition to an entirely different mode of behavior.

B. Symmetry-breaking fields

From the experimental point of view, our most important results relate to the effect of symmetry-breaking fields like h_p. In recent years, it has become possible to study experimentally critical phenomena in crystals which are effectively two-dimensional. Indeed, Birgeneau *et al.*[20] have measured critical exponents for the Ising-like quasi-two-dimensional antiferromagnetic K_2NiF_4 which are strikingly similar to those expected for the two-dimensional Ising model.

One might hope that similar substances with the XY symmetry of the planar model could also be studied experimentally.[21] However real magnetic crystals are subject to symmetry-breaking crystalline fields in addition to an isotropic exchange coupling. Thus, one must consider the more general Hamiltonian (1.1) with at least one of the h_p's nonzero. In practice, we expect to encounter crystalline anisotropies with $p = 2-4$ and 6. The effect of an applied external magnetic field is given by $p = 1$.

Although Eq. (1.1) is difficult to analyze directly, we may form conclusions about the h_p perturbations both from the Migdal scheme and also from the generalized Villain model. The Migdal scheme implies that as $T \to 0$ all h_p perturbations are strongly relevant variables. Recursion by recursion, an h_p perturbation will grow and grow finally forcing the system into a state of broken symmetry in which one of the directions $\theta = 2\pi n/p, n = 0, 1, \ldots, p-1$, is especially preferred. Thence any h_p perturbation will force the system away from a planar model behavior if T is sufficiently small.

The generalized Villain model then gives a precise meaning to "sufficiently small" T. If this model lies in the same universality class as the planar model, then a small perturbation with in-

dex p will be relevant if

$$8\pi K_{eff} > p^2 . \tag{1.5}$$

If this inequality is satisfied, the planar model system will be unstable against ordering via h_p-type perturbations. Equations (1.4) and (1.5) then imply together that the Gaussian spin-wave behavior of the planar model (and its universality "cousins") is stable against symmetry-breaking perturbations and destruction via vortices provided

$$4 < 2\pi K_{eff} < \tfrac{1}{4} p^2 . \tag{1.6}$$

There is no such stability region for uniaxial perturbations ($p = 2$) or triangular perturbations ($p = 3$). The square perturbations have a vanishing stability region. But a real planar system with hexagonal perturbation may be expected to show typical critical planar model behavior for

$$4 < 2\pi K_{eff} < 9 .$$

We hope that experimentalists will attempt to find and study such a system.

Phase diagrams for $p = 6$ and $p = 4$ are shown in Fig. 1. The lines of asterisks at $h_p = 0$ indicate the Kosterlitz-Thouless line of critical points with continuously variable exponents. On lowering the temperature of fixed $h_p \neq 0$, one first crosses an upper critical temperature $T_1(h_6)$ into a planar model "phase" of critical points with continously variable exponents. There is a second transition at temperature $T_2(h_6)$ into a discrete planar ordered phase, where the system orders into one of the six preferred directions selected by the symmetry-breaking perturbation. The susceptibility diverges exponentially fast [i.e., as in Eq. (5.7)] on approaching $T_1(h_6)$ from above or $T_2(h_6)$ from below, and remains infinite between these temperatures. For the Villain models considered here, we find $\eta = \frac{1}{4}$ as T goes to $T_1(h_6)$ from below and $\eta = \frac{1}{9}$ as T tends to $T_2(h_6)$ from above.

The predictions for $p = 4$ are also rather striking. The three lines of critical points shown in Fig. 1(b) correspond to three distinct lines of fixed points! Thus, they are denoted by asterisks to show that all three display continuously variable exponents. The second-order phase transition into an ordered four-state phase for $h_4 \neq 0$ should display conventional power law singularities, but with *nonuniversal* critical exponents. Although we find $\eta = \frac{1}{4}$ at the confluence of these critical lines, we have not completely reconciled this result with the predictions of Luther and Scalapino[13] (see Sec. V).

The stability of various h_p perturbations was analyzed previously within spin wave theory by Prokrovsky and Uimin,[22] while Kosterlitz and Thouless have shown how this analysis is modified by vortices in a recent review article.[23] Both sets of authors suggested that there would be two phase transitions for $p > 4$. In Sec. V C, we present a nonlinear recursion analysis which refines and considerably sharpens this picture. The results lead directly to the phase diagrams shown in Fig. 1, and allow detailed predictions to be made about the associated critical behavior for small h_p. We have been unable to ascertain the small h_p structure of the phase diagrams for $p = 2$ and $p = 3$.[24]

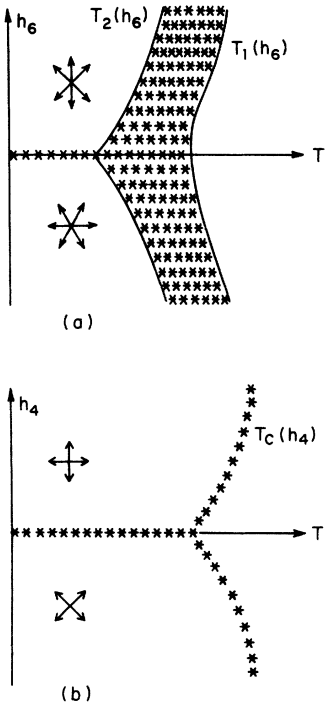

FIG. 1. Phase diagrams in the h_p-T plane for $p = 6$ and $p = 4$. The asterisks denote critical points with continuously variable critical exponents.

As pointed out by Kosterlitz and Thouless,[23] isotropic planar behavior should be very difficult to see experimentally in quasi-two-dimensional magnetic systems, because of an unusually strong crossover to three-dimensional behavior. Hopefully, experimental analogues of the models studied here can be found elsewhere in nature, perhaps in systems exhibiting nonmagnetic phase transitions.

C. Outline

In Sec. II we discuss various transformations on the action (1.1) which are useful both in the context of the Migdal approximation and in the analytic treatment. Section III describes the results which can be obtained from the Migdal recursion

relation, both with and without symmetry-breaking perturbations. In Sec. IV we demonstrate explicitly that the generalized Villain model collapses readily into the Coulomb gas system treated by Kosterlitz and determine the first correction to the Berezinskii results in a cumulant expansion. Finally, in Sec. V we rederive results obtained by Kosterlitz, and present a more detailed analysis of symmetry-breaking perturbations. We also summarize our conclusions and speculations about the isotropic planar model at this point. Appendix A shows how symmetry-breaking fields can be treated within the spin-wave approximation, and Appendix B discusses a generalization of the Migdal approach which allows for symmetry-breaking interactions. Appendix C explains certain features of the cumulant expansion of Sec. IV, whereas Appendix D proves a duality transformation result given in Sec. V B.

II. TRANSFORMATIONS OF THE ACTION

A. Fourier analysis and the Villain model

The planar model has a coupling between nearest-neighbor "spins" of the form

$$V(\theta-\theta')=-K[1-\cos(\theta-\theta')]\,. \tag{2.1}$$

Of course a periodic function like this can always be written in a Fourier series

$$e^{V(\theta)}=\sum_{s=-\infty}^{\infty} e^{is\theta+\tilde{V}(s)}\,, \tag{2.2}$$

where the Fourier coefficient is given by

$$e^{\tilde{V}(s)}=\int_0^{2\pi}\frac{d\theta}{2\pi}\,e^{-is\theta+V(\theta)}\,. \tag{2.3}$$

The coupling (2.1) has $\tilde{V}(s)$ given in terms of a Bessel function of imaginary argument

$$e^{\tilde{V}(s)}=e^{-K}I_s(K)\,. \tag{2.4}$$

In the limit of large and small couplings this reduces to

$$e^{\tilde{V}(s)}=\begin{cases}(1/s!)(\frac{1}{2}K)^s\,, & K\to 0\,,\\ e^{-s^2/2K}/(2\pi K)^{1/2}\,, & K\to\infty.\end{cases} \tag{2.5}$$

For small K the sum in Eq. (2.2) converges quite rapidly with only the $s=0$ and ±1 terms contributing. However, for large K the summation converges very slowly. To get a more rapidly converging result, we use the Poisson summation formula, which in its simplest form states that the sum over s of any function $g(s)$ can be written

$$\sum_{s=-\infty}^{\infty} g(s)=\sum_{m=-\infty}^{\infty}\int_{-\infty}^{+\infty} d\phi\, g(\phi)e^{-2\pi i m\phi}\,. \tag{2.6}$$

Hence, Eq. (2.2) can be rewritten in terms of a sum over m as

$$e^{V(\theta)}=\sum_m e^{V_0(\theta-2\pi m)}\,, \tag{2.7}$$

where V_0 is given as a Fourier integral

$$e^{V_0(\theta)}=\int d\tilde{\phi}\, e^{\tilde{V}(\tilde{\phi})+i\tilde{\phi}\theta}\,. \tag{2.8}$$

At low temperatures the sum over m in Eq. (2.7) will converge quite rapidly. In fact, the integers m in this formula will describe the quantum numbers of vortices in the system, while the integration variable ϕ in Eq. (2.8) will represent the spin waves.

Notice that the summation over m in Eq. (2.7) automatically enforces the periodicity of $V(\theta)$. Hence, V_0 may itself be a nonperiodic function. The simplest choice of V_0 was made by Villain[17] who took

$$V_0(\theta)=-\tfrac{1}{2}K_V\theta^2\,, \tag{2.9a}$$

which implies the simple Gaussian form for $\tilde{V}(\tilde{\phi})$

$$\tilde{V}(\tilde{\phi})=-\tilde{\phi}^2/2K_V\,. \tag{2.9b}$$

In Sec. III we arrive at the Villain coupling in a different way. The Migdal procedure starts from any interaction function between nearest-neighbor spins—say the interaction (2.1)—and replaces it with a new interaction function $V'(\theta-\theta')$ generated from an approximate decimation renormalization-group transformation. After a few iterations of this procedure, we find that any interaction function at reasonably low temperatures appears to generate a new interaction of the form

$$e^{V_V(\theta-\theta')}=\sum_{m=-\infty}^{\infty} e^{-K_V(\theta-\theta'-2\pi m)^2/2}\,, \tag{2.10}$$

with $K_V\approx K$. This correspondence is important because (2.10) is the model proposed by Villain,[17] which does have some properties which are much simpler than those of the original planar model. The Migdal-style analysis suggests that the two interaction models can indeed have very similar critical properties.

In particular, we suggest that the critical properties of the two models will be identical if we choose K_V to be some function of K:

$$K_V=f(K)\,.$$

A comparison of the interaction form for weak and strong couplings show them to be identical if

$$f(K)=\begin{cases}K & \text{for } K\to\infty,\\ [2\ln(2/K)]^{-1} & \text{for } K\to 0\,.\end{cases} \tag{2.11}$$

B. Duality transformations

We can make use of the tricks described in Sec. II A to perform a duality transformation on a pla-

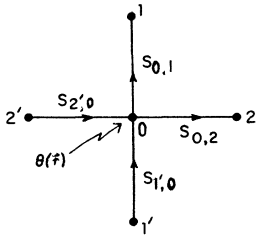

FIG. 2. Five vertices of a square lattice populated with "angle" variables $\theta(\vec{r})$. Four integer variables s populate the bonds connecting to the central vertex. The arrows suggest our convention for ordering adjacent θ variables in the Fourier transform of the nearest-neighbor potential.

nar model with arbitrary nearest-neighbor interaction. That is, we consider an action of the form

$$A[\theta]=\sum_{\langle\vec{r},\vec{r}'\rangle} V(\theta(\vec{r})-\theta(\vec{r}')) \tag{2.12}$$

entering a partition sum

$$Z=\int d[\theta]e^{A[\theta]}=\left(\prod_{\vec{r}}\int_0^{2\pi}\frac{d\theta(\vec{r})}{2\pi}\right)e^{A[\theta]}. \tag{2.13}$$

For definiteness, imagine that the sums run over the sites of a square lattice, although the transformations described below are easily generalized.

The first step is to write every term in $A[\theta]$ as an expansion of the form (2.1). In writing (2.1) for a particular lattice bond, we shall always choose θ to be either to the left of or below θ'. These substitutions yield a partition function which depends both on the angle $\theta(\vec{r})$ at a lattice site and on integers $S(\vec{r},\vec{r}')$ which populate the lattice bonds:

$$Z=\int d[\theta]\prod_{\langle r,r'\rangle}\sum_{S(\vec{r},\vec{r}')=-\infty}^{\infty}\exp\{\tilde{V}(S(\vec{r},\vec{r}'))+iS(\vec{r},\vec{r}')\times[\theta(\vec{r})-\theta(\vec{r}')]\}. \tag{2.14}$$

The θ integrals can be performed immediately. A typical integral is represented by Fig. 2. The $e^{is\theta}$ terms just give Kronecker δ functions restricting the sums over s. For example, the case shown in Fig. 2 gives

$$\Delta(\vec{r})\equiv\delta_{S_{0,1}+S_{0,2}+S_{1',0}+S_{2',0}}. \tag{2.15}$$

Thus, Z reduces to a sum over bond variables $S(\vec{r},\vec{r}')$ with a set of δ function symbols at every site:

$$Z=\sum_{\{S(r,r')\}}\left(\prod_{\vec{r}}\Delta(\vec{r})\right)\exp\sum_{\langle\vec{r},\vec{r}'\rangle}\tilde{V}(S(\vec{r},\vec{r}')). \tag{2.16}$$

For a lattice of N sites, there are clearly $2N$ summation variables and N restrictions represented by the $\Delta(\vec{r})$'s. The restrictions can be thought of as requirements that the net $S(\vec{r},\vec{r}')$ "flowing" into any site vanish. This "zero divergence" condition can, in fact, be met by choosing the $S(\vec{r},\vec{r}')$ field to be the "curl" of a new field $S(\vec{R})$. With this in mind, we choose a new set of integer variables $\vec{S}(\vec{R})$ defined at the centers of the cells of the old lattice. A set of four cells is shown in Fig. 3.

Now make the ansatz that each $S(\vec{r},\vec{r}')$ can be written in terms of differences of the $S(\vec{R})$:

$$\begin{aligned}&S_{0,1}=S_A-S_B,\quad S_{0,2}=S_B-S_C,\\&S_{1',0}=S_D-S_C,\quad S_{2',0}=S_A-S_D.\end{aligned} \tag{2.17}$$

With this new set of variables, the $N\Delta(\vec{r})$ constraints are satisfied automatically, and the $2N$ sums become N unconstrained sums over the variables $S(\vec{R})$ populating the dual lattice. The function $\tilde{V}(S(\vec{r},\vec{r}'))$ now becomes a nearest neighbor coupling $V(S(\vec{R})-S(\vec{R}'))$ between these new variables. We are left with the problem of evaluating

$$Z[S]=\sum_{\{S(\vec{R})\}}\exp\left(\sum_{\langle\vec{R},\vec{R}'\rangle}\tilde{V}(S(\vec{R})-S(\vec{R}'))\right), \tag{2.18}$$

where each $S(\vec{R})$ is summed over the set of integers.[18]

Equation (2.18) is an exact rewriting of the partition function. Unfortunately, we do not have much experience in statistical mechanics in evaluating sums of this kind. Furthermore, we do not expect the sums in (2.18) to converge very rapidly at low temperatures. Both difficulties can be eliminated by performing the transformation (2.6) on each $S(\vec{R})$ sum to obtain

$$Z=\sum_{\{m(\vec{R})\}}\left(\prod_{\vec{R}}\int_{-\infty}^{\infty}d\phi(\vec{R})\right)\exp\left(\sum_{\langle\vec{R},\vec{R}\rangle}\tilde{V}(\phi(\vec{R})-\phi(\vec{R}'))+\sum_{\vec{R}}2\pi im(\vec{R})\phi(\vec{R})\right). \tag{2.19}$$

Equation (2.19) is our final result for the partition function. As we shall see, $\phi(\vec{R})$ describes the spin-wave degrees of freedom, while $m(\vec{R})$ is a quantum number for a vortex excitation. In the limit of low temperatures, the sums over $m(\vec{R})$ should converge quite rapidly.

C. Dual transformations on correlation functions

Similar tricks can be used to transform correlation functions, e.g.,

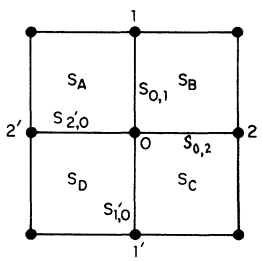

FIG. 3. Representation of the bond integers variable by integer variables on the dual lattice whose "curl" automatically satisfies the divergence condition.

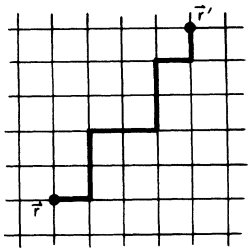

FIG. 4. Bonds entering the representation of the correlation function $g_p(\vec{r}-\vec{r}')$.

$$g_p(\vec{r}-\vec{r}') \equiv \langle e^{ip[\theta(\vec{r})-\theta(\vec{r}')]}\rangle, \tag{2.20}$$

where p is an integer. The expectation is to be taken in the ensemble specified by the action (2.12). With $p=1$, the real part of (2.20) is just the average of the vector product of two spins located at sites $\vec{r}$ and $\vec{r}'$. The other values of p are related to various symmetry-breaking perturbations, as we shall see.

First, imagine we wish to determine $Zg_p(\vec{r}-\vec{r}')$, where $\vec{r}$ and $\vec{r}'$ are nearest-neighbor sites. Dual transformations on this object carry through exactly as before, except that the bond connecting r and r' has a new statistical weight, namely

$$e^{V'(\theta(\vec{r})-\theta(\vec{r}'))} = e^{V(\theta(\vec{r})-\theta(\vec{r}'))}e^{ip[\theta(\vec{r})-\theta(\vec{r}')]}$$

$$= \sum_s \exp\{is[\theta(\vec{r})-\theta(\vec{r}')] + \tilde{V}(s-p)\}. \tag{2.21}$$

Thus, the effect of the factor $e^{ip[\theta(\vec{r})-\theta(\vec{r}')]}$ is to shift the argument in one of the $\tilde{V}$ by an amount p. The conclusion is that in the nearest-neighbor case

$$g_p(\vec{r}-\vec{r}') = Z'/Z, \tag{2.22}$$

where Z is given by (2.18), and Z' has a similar form,

$$Z' = \sum_{\{S(\vec{R})\}} \exp\Big(\sum_{\langle \vec{R},\vec{R}'\rangle} \tilde{V}(S(\vec{R}) - S(\vec{R}') - \eta_{\vec{R}\vec{R}'}p)\Big). \tag{2.23}$$

Here $\eta_{\vec{R}\vec{R}'}$ is a "projection operator" which is unity on the dual image of the special nearest-neighbor bond and zero everywhere else.

Now consider correlations over longer distances An expression such as (2.20) can be written as the average of a product of nearest-neighbor terms $e^{ip[\theta(\vec{r})-\theta(\vec{r}')]}$. For example, the correlation shown in Fig. 4 can be represented as a product

$$Z' \equiv \langle e^{ip[\theta(\vec{r}_0)-\theta(\vec{r}_N)]}\rangle = Z\Big\langle \prod_{j=0}^{N} e^{ip[\theta(\vec{r}_j)-\theta(\vec{r}_{j+1})]}\Big\rangle. \tag{2.24}$$

Consequently, a path can be chosen running from $\vec{r}_0$ to $\vec{r}_N$ as shown in Fig. 4, and the Z' of Eq. (2.24) can be calculated as in the nearest-neighbor case. The result is that Z' has the form (2.23) but with the projection operator $\eta_{\vec{R},\vec{R}'}$, given by

$$\eta_{\vec{R},\vec{R}'} = \begin{cases} 0 & \text{if the path does not cut the bond } \vec{R}\vec{R}', \\ +1 & \text{if } \vec{R} \text{ lies just to the left of the path and } \vec{R}' \text{ just to the right,} \\ -1 & \text{if } \vec{R}' \text{ lies just to the left of the path and } \vec{R} \text{ just to the right.} \end{cases} \tag{2.25}$$

Or employing the Poisson sum formula once again, we obtain our final result

$$g_p(\vec{r}-\vec{r}') = Z^{-1}\Big(\prod_{\vec{R}} \int_{-\infty}^{\infty} d\phi(\vec{R})\Big) \sum_{\{m(\vec{R})\}} \exp\Big(\sum_{\langle \vec{R},\vec{R}'\rangle} \tilde{V}(\phi(R) - \phi(\vec{R}') - \eta_{\vec{R}\vec{R}'}p) + 2\pi i \sum_{\vec{R}} m(R)\phi(\vec{R})\Big). \tag{2.26}$$

III. MIGDAL APPROXIMATION

A. Isotropic planar model recursion relation

The Migdal recursion scheme[15] has recently been reviewed and rederived by a potential-moving technique.[25] It is this potential-moving point of view we will take here.

We first review the decimation recursion relations for the isotropic planar model (1.1) (with all h_p's set to zero) in one dimension; that is, we explicitly integrate out the angle variables at every other site in a linear chain. It is easily shown[15,25] that the Fourier components of an arbitrary nearest-neighbor potential obey an exact recursion formula

$$\tilde{V}'(s) = 2\tilde{V}(s), \tag{3.1}$$

where $\tilde{V}'(s)$ represents the new Fourier component obtained after decimation. If $b-1$ out of b sites are summed over the resulting interaction is

$$\tilde{V}'(s) = b\tilde{V}(s). \tag{3.2}$$

The Migdal approach can be viewed as a procedure for bootstrapping equations like (3.2) into higher dimensions.[25] The basic ideas are summarized in Fig. 5. First one moves the vertical bonds in every row of a square lattice, as shown in Fig. 5(b). The spins indicated by an × in Fig. 5(b) are then removed by a one-dimensional decimation to give Fig. 5(c). Finally, the lattice is rotated by 90° and the entire operation is repeated. We refer the reader to the literature for a detailed discussion of the validity of this procedure.

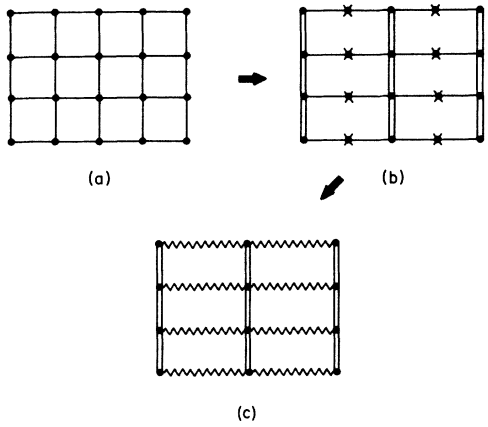

FIG. 5. One half of the Migdal transformation on a two-dimensional lattice. New vertical bonds are obtained by moving every other vertical bond on top of a remaining bond. New horizontal bonds are then obtained by decimating out the isolated vertices.

For any $b>1$, this interpretation of the Migdal scheme introduces anisotropic horizontal and vertical couplings, even if these are initially identical.[25] Thus, it is necessary to consider recursion relations for both x- and y-direction nearest-neighbor Fourier components $\tilde{V}_x(s)$ and $\tilde{V}_y(s)$. These recursion relations are

$$e^{\tilde{V}_x'(s)}=\frac{1}{2\pi}\int_0^{2\pi}d\theta\, e^{-is\theta}\Big(\sum_{s_i} e^{is_1\theta}e^{bV_x(s_1)}\Big)^b, \tag{3.3a}$$

$$e^{\tilde{V}_y'(s)}=\Big[\frac{1}{2\pi}\int_0^{2\pi}d\theta\, e^{-is\theta}\Big(\sum_{s_i} e^{is_1\theta}e^{\tilde{V}_y(s_1)}\Big)^b\Big]^b . \tag{3.3b}$$

The new interactions in real space can be recovered by summing a Fourier series

$$e^{V_x'(\theta)}=\sum_s e^{is\theta}e^{\tilde{V}_x'(s)}, \tag{3.4a}$$

$$e^{V_y'(\theta)}=\sum_s e^{is\theta}e^{\tilde{V}_y'(s)}. \tag{3.4b}$$

Note the symmetry between the recursion formulas for the x and y bonds: To obtain the x recursion (with, say, $b=2$) we first double the interaction in Fourier space, and then double the interaction in real space. To obtain the y recursion, we perform these same operations in the reverse order.

The Migdal recursion relation becomes isotropic as $b\to 1$, so it is of interest to consider (3.3) in this limit. On expanding in $b-1\simeq \ln b$, we obtain recursion relations for a single isotropic set of Fourier coefficients

$$\frac{de^{V(s)}}{dl}=V(s)+\frac{1}{2\pi}\int_0^{2\pi}d\theta\, e^{-is\theta}\Big(\sum_{s_1} e^{is_1\theta}e^{V(s_1)}\Big)\times\ln\Big(\sum_{s_2} e^{is_2\theta}e^{V(s_2)}\Big), \tag{3.5}$$

where

$$l\equiv\ln b \tag{3.6}$$

is the logarithm of the change in length scale. Although it is isotropic, this set of equations is rather difficult to work with. Equations (3.3) (with integer b) are easier to treat with high precision on a computer. The bulk of our numerical calculations were done on Eq. (3.3b), with $b=2$, which can be rewritten as a single summation

$$e^{\tilde{V}_y'(s)}=\Big(\sum_{s_1} e^{\tilde{V}_y(s_1)}e^{\tilde{V}_y(s-s_1)}\Big)^2. \tag{3.7}$$

B. Numerical analysis and fixed points

Given functional recursion relations such as (3.3) or (3.7), we want to follow the progress under repeated iterations of various initial interaction functions. Of course, fixed points are of particular interest. An infinite temperature fixed point would correspond to an interaction independent of θ, $V(\theta)=\text{const}$. A zero-temperature fixed-point function would be infinite everywhere except at $\theta=0$ or 2π, on a scale chosen such that $V(\theta=0)=0$.

Figure 6 illustrates what happens to an initial interaction

$$V_y(\theta)=K(1-\cos\theta). \tag{3.8}$$

After three or four iterations of the transformation (3.7), a limiting function is apparently reached which depends on the initial coupling K in (3.8). Limiting fixed-point functions are shown for $K^{-1}=0.5$ and 0.8. These functions are periodic in θ, although certainly not cosines, and are approached for all $K\geq 1$. For $K\leq 1$, any initial function tends toward a high-temperature fixed point. Very similar behavior was found for (3.3a) with $b=2$. These qualitative properties of the transformation (3.3) were first discovered by Migdal.[15]

If the planar model had a conventional critical point in two dimensions, we would expect a single isolated unstable fixed point, in addition to the zero- and infinite-temperature fixed points. However, the behavior described in the preceding paragraph suggests that the planar model has a line of fixed points at low temperatures. This indicates the existence of a line of critical points, with continuously variable critical exponents. Clearly, it is important to investigate this point further.

To help visualize what is at issue, we have sum-

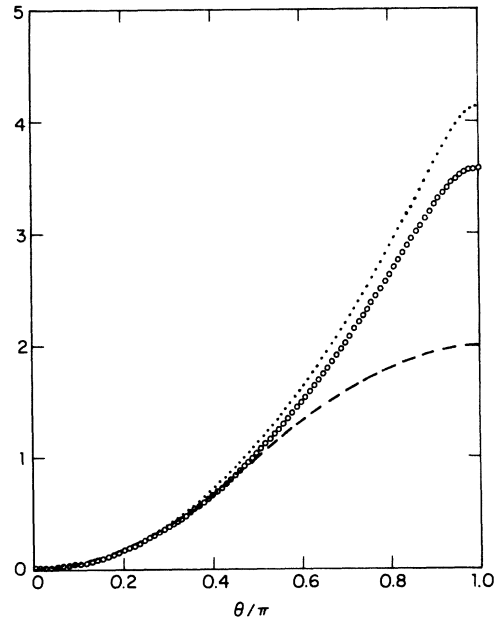

FIG. 6. Invariant interaction functions $V_x(\theta)$ approached by the Migdal transformation for initial interaction strengths $K^{-1}=0.5$ (dots) and $K^{-1}=0.8$ (circles). The initial interaction functions are proportional to $1-\cos\theta$ (dashed line).

marized the properties of the interaction functions at each iteration by just two parameters, an effective "temperature" T_{eff} and a barrier height B given by

$$T_{eff}^{-1}=\left.\frac{-d^2V(\theta)}{d\theta^2}\right|_{\theta=0}=\sum_s s^2e^{V(s)}\Big/\sum_s e^{V(s)} \tag{3.9}$$

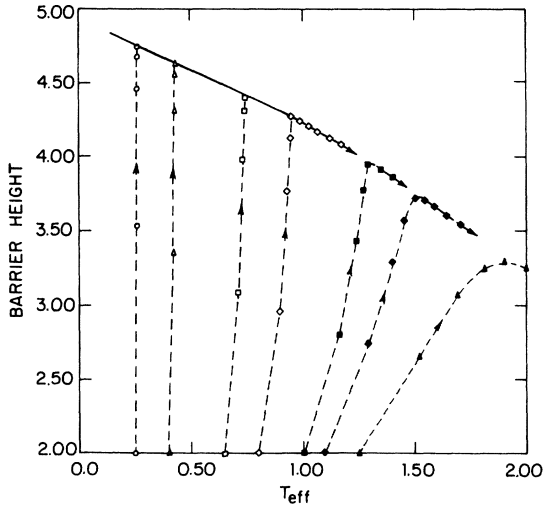

FIG. 7. The Migdal transformation parametrized by an effective temperature and barrier height. The circles, triangles, etc., indicate iterations of the $b=2$ transformation from the line of barrier height =2.0.

$$B=T_{eff}[V(\theta=0)-V(\theta=\pi)]. \tag{3.10}$$

For the interaction (3.8), $T_{eff}=K^{-1}=k_BT/J$, and $B=2.0$ initially. The renormalization flows in (T_{eff},B) space are shown in Fig. 7. Initial interactions with $B=2.0$ and $T_{eff}\leq 0.8$ iterate rapidly to an apparent fixed line. For $T_{eff}\geq 0.8$, the iterations eventually bend toward high temperatures and low barriers along a universal trajectory.

Let us try to guess the approximate fixed-point function which is approached for $T_{eff}\leq 0.8$. It turns out that the Villain model is an extremely good guess. On substituting the ansatz

$$e^{\tilde{V}(s)}=e^{-s^2/2K_V} \tag{3.11}$$

into Eqs. (3.3a) or (3.3b) and approximating the sums by integrals, we obtain

$$e^{\tilde{V}'(s)}=\text{const}\times e^{-s^2/2K_V}. \tag{3.12}$$

Absorbing the constant into a redefinition of the free energy, we see that the s dependence of the new interaction is identical to the old. In Fig. 8, we compare various apparent fixed-point functions found by iterating (3.7) with the Villain model for an appropriately chosen K_V. The Villain model is a rather accurate representation for all $T_{eff}\leq 0.8$, corresponding to the apparent fixed line in Fig. 6.

Unfortunately, the Villain model does not actually

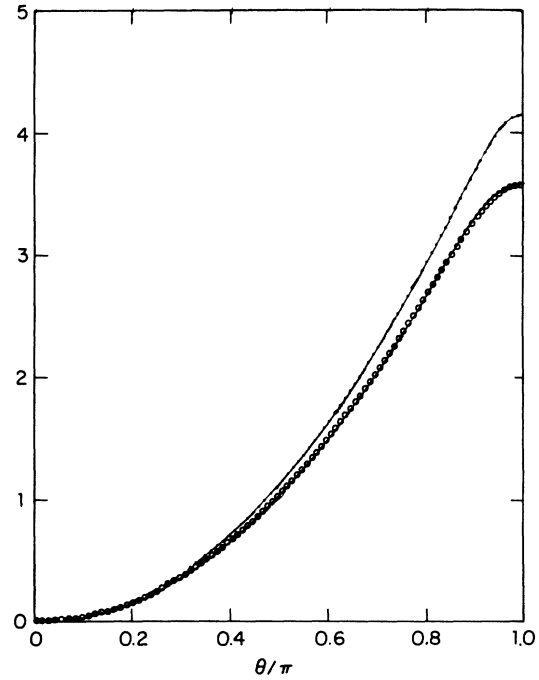

FIG. 8. Comparison of apparent fixed-point functions found with the Migdal transformation, and an appropriately chosen Villain model for $K^{-1}=0.5$ (dots) and $K^{-1}=0.8$ (circles).

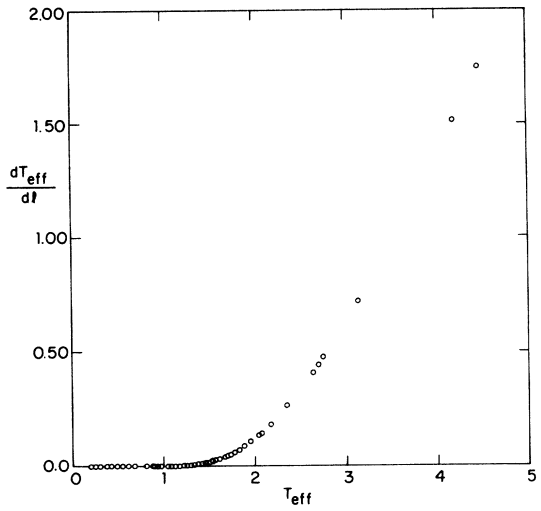

FIG. 9. Change in effective temperature with iteration dT_{eff}/dl for the Migdal transformation. This quantity is almost identically zero until $T_{eff} \simeq 1.0$.

represent a family of exact fixed-point functions of the Migdal transformation. We can see this, for example, by calculating the error introduced at low temperatures in Eq. (3.7) by approximating the sum by an integral

$$e^{\tilde{V}'_x(s)} = \sum_{s_1=-\infty}^{\infty} e^{-s_1^2/K_V} e^{-(s-s_1)^2/K_V}$$

$$= \sum_{m=-\infty}^{\infty} \int_{-\infty}^{+\infty} d\phi\, e^{-\phi^2/K_V} e^{-(s-\phi)^2/K_V} e^{2\pi i m\phi}$$

$$= (\tfrac{1}{2}\pi K_V)^{1/2} e^{-s^2/2K_V}[1 + 2\cos(\pi s) e^{-\pi^2 K_V/2}] \,. \tag{3.13}$$

The Villain model fails exponentially to be a fixed point.

To see if there really is a one-parameter family of fixed-point functions (which is presumably "close" to a family of Villain models), we investigate very precisely changes in the effective temperature with iteration. Consider the quantity

$$\frac{dT_{eff}}{dl} \equiv \frac{T'_{eff} - T_{eff}}{\ln 2} \tag{3.14}$$

for the transformation (3.7); this should be identically zero along a fixed line. In Fig. 9 we have plotted dT_{eff}/dl along the apparent fixed line versus T_{eff}. The change in T_{eff} appears to be identically zero until $T_{eff} \simeq 1.0$, which would be consistent with a fixed line. However, appearances can be deceiving. In Fig. 10, $\log_{10}(dT_{eff}/dl)$ is plotted against $1/T_{eff}$. The "differential" change dT_{eff}/dl decreases exponentially in $1/T_{eff}$ over at least 20 decades! To a good approximation,

$$\frac{dT_{eff}}{dl} = 79.4 e^{-13.2/T_{eff}} \tag{3.15}$$

at low temperatures, suggesting that dT_{eff}/dl is positive for all nonzero temperatures and that there is no phase transition.

This conclusion, that there is almost, but not quite a fixed line within the Migdal approximation, was reached previously by Wilson,[19] who showed analytically that

$$\frac{dT_{eff}}{dl} \sim \exp(-4\pi^2/3T_{eff}) \tag{3.16}$$

at low temperatures. The number $\frac{4}{3}\pi^2$ is very close to 13.2.

It is interesting to contrast the Migdal approximation to the planar model, summarized in Fig. 10 with the corresponding quantity for the two-dimensional Ising model, shown in Fig. 11. Within the Migdal scheme, it is known analytically that[15,25]

$$\frac{dT_{eff}}{dl} = -T_{eff} - \frac{T_{eff}^2 \tanh(1/T_{eff}) \ln[\tanh(1/T_{eff})]}{1 - \tanh^2(1/T_{eff})}, \tag{3.17}$$

where $T_{eff} = k_B T/J$ in this case. The Migdal transformation does predict rather bizarre behavior for the planar model at $T = 0$. Given the form (3.15) it is possible to show that the susceptibility diverges as the exponential of an exponential as $T \to 0$,

$$\chi \sim \exp(A T^2 e^{B/T}) \,, \tag{3.18}$$

where A and B are constants. Similar behavior has

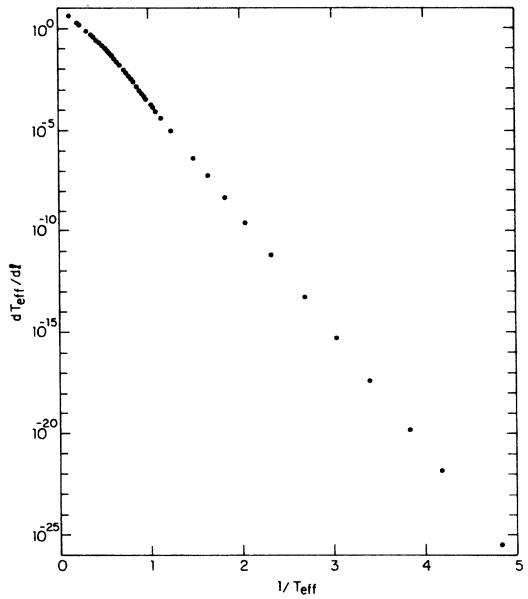

FIG. 10. Plot of dT_{eff}/dl vs $1/T_{eff}$. The graph is linear over about 20 decades in dT_{eff}/dl.

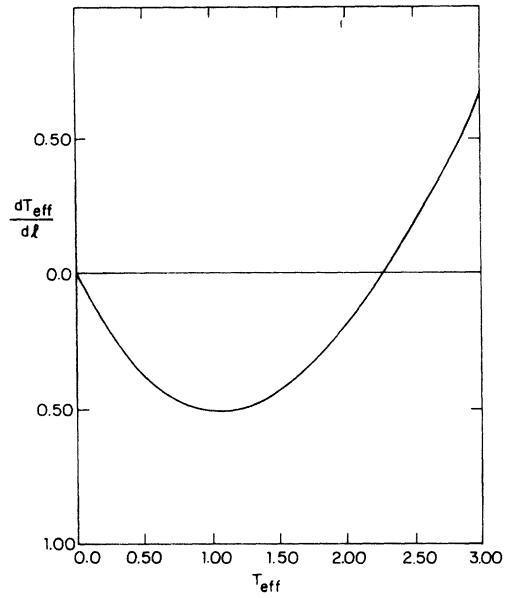

FIG. 11. Differential recursion relation $dT_{eff}/d\ell$ obtained from Migdal's recursion formula for the two-dimensional Ising model.

been found in the correlation length of a "truncated tetrahedron" Ising model.[26]

We do not yet know if we should believe the detailed predictions of the Migdal theory. Although the rapid approach of an initial interaction to something resembling a Villain model is probably qualitatively correct, we shall suggest in Sec. IV that the approximation does not treat vortices properly along the apparent fixed line. In any event, it is clear from Fig. 9 that the Migdal approach simulates a fixed line remarkably well, as first observed by Migdal himself.[14]

C. Symmetry-breaking interactions

We now investigate the symmetry-breaking perturbations displayed in Eq. (1.1). In Appendix A we deduce the renormalization-group eigenvalues of these fields along the fixed line in the spin-wave approximation. A small field h_p should obey the recursion law

$$h_p' \simeq b^{\lambda_p(T)} h_p, \tag{3.19}$$

with

$$\lambda_p(T) = 2 - (k_B T/4\pi J)p^2. \tag{3.20}$$

Apparently, the h_p variables should be strongly *relevant* at low temperatures ($\lambda_p > 0$). An initially small crystalline field will grow rapidly, leading to behavior quite different from that found for $h_p = 0$. However, (3.20) also suggests that some of these fields may become *irrelevant* ($\lambda_p < 0$) at sufficiently high temperatures. The h_p's would then become smaller with iteration, and would not affect the isotropic planar model behavior. The borderline between relevancy and irrelevancy of a particular field h_p occurs at a temperature

$$k_B T_m = 8\pi J/p^2. \tag{3.21}$$

At $T = T_m$, the eigenvalue is *marginal* ($\lambda_p = 0$).

We first want to calculate the $\lambda_p(T)$ in the framework of the Migdal theory. The spin-wave approximation is certainly suspect at higher temperatures, although it does suggest that $\lambda_6(T)$ is more likely to become irrelevant than $\lambda_2(T)$. The second aim of this section will be to investigate the critical behavior which occurs if the $\lambda_p(T)$ are relevant. We have done this numerically, and have relegated the necessary generalization of the Migdal scheme to Appendix B.

The characteristic behavior of $\lambda_p(T)$ in the Migdal approximation can be seen by carrying out a one-dimensional decimation with $h_p \neq 0$ for some p, approximating $V(\theta)$ by a Gaussian $-\theta^2/2T_{eff}$ and expanding to first order in h_p. The result

$$h' = h(1 + e^{-p^2 T_{eff}/4}) \quad \text{for } b = 2 \tag{3.22}$$

gives $\lambda_p > 0$ for all p and T_{eff}. Combining (3.22) with a bond-shifting transformation, as described in Appendix B, we obtain the eigenvalues $\lambda_p(T)$ for $p = 1$–4 and 6 shown in Fig. 12.

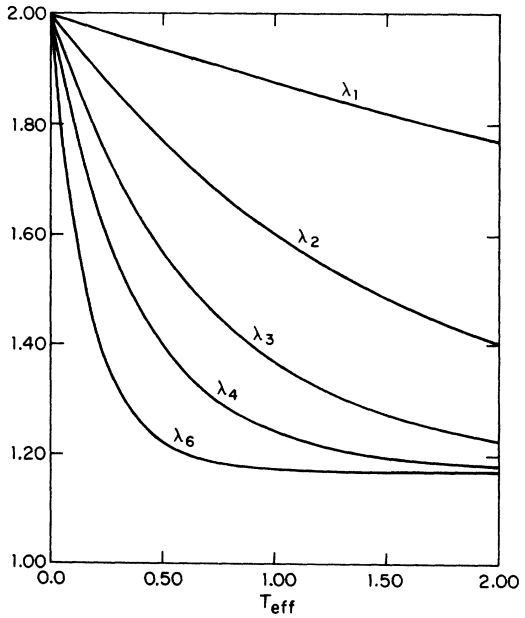

FIG. 12. Eigenvalues $\lambda_p(T)$ of various symmetry-breaking perturbation along the apparent fixed line in the Migdal recursion relation.

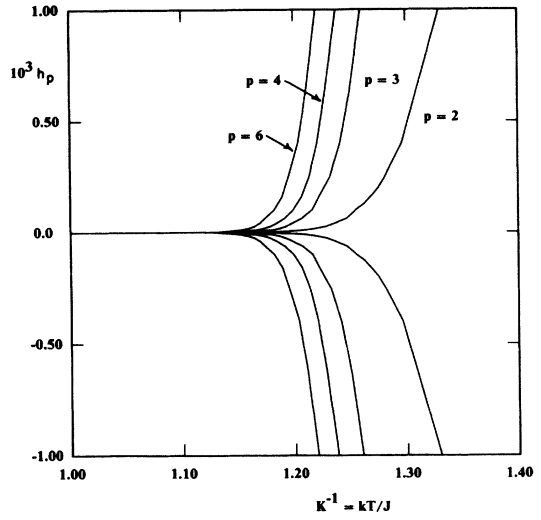

FIG. 13. Phase diagrams in the $h_p - K^{-1}$ plane for $p = 2, 3, 4$, and 6 as given by Migdal transformation. The lines are lines of second-order phase transitions with exponents characteristic of a p-state planar model.

At low temperatures $\lambda_p(T)$ decreases from 2.0 in proportion to p^2T for all p, and all eigenvalues saturate at the same value at high temperatures. This high-temperature limit depends upon the scale factor b and the free parameter α whose choice is discussed in Appendix B. For all physically sensible values of b and α, the Migdal scheme gives $\lambda_p(T) \geq 0$ as $T \to \infty$. We shall see in Sec. IV that $\lambda_p(T)$ actually does go negative at rather low temperature for $p > 4$, although the Migdal approximation may be qualitatively correct for $p = 1-3$.

We have also tracked the effective interactions which result as the h_p's iterate toward larger values (in Secs. IV and V, we will only be able to treat the small-h_p limit). It appears that the on-site potentials h_p become unboundedly large with many iterations of the Migdal recursion relation. Consequently, the Hamiltonian (1.1) (with a single nonzero h_p) rapidly becomes equivalent to a planar model with p discrete allowed states.

As discussed in Sec. IIID, we expect these p-state models to have at least one phase transition as the temperature is varied[27] for $p \geq 2$ ($p = 2$ is an Ising model). Thus an h_p-K^{-1} plane of initial Hamiltonians divides into two regions, one which maps under the Migdal transformation into a p-state model above its critical point, and one which goes into a p-state model below T_c. The phase boundaries obtained in this way for $p = 2-4$ and 6 are shown in Fig. 13. Each curve is a line of second- (or possibly first) order phase transitions with exponents appropriate to the corresponding p-state planar model. For small h_p and $K^{-1} = k_B T$ these lines are given by

$$h_p \sim e^{-AT^2 e^{B/T}}, \tag{3.22}$$

where A and B are constants. This prediction is consistent with the zero critical temperature found earlier for the isotropic planar model in this approximation.

We emphasize that there are strong reasons to suspect the phase boundaries shown in Fig. 13 for $p \geq 4$ (see the Introduction and Sec. V). The plots for $p = 2$ and $p = 3$ may be qualitatively correct, however.

D. Discrete planar models

Motivated by the numerical results of Sec. IIIC, we consider the limiting case of the discrete models which are approached by (1.1) after many iterations. For simplicity imagine taking one of the h_p's infinite and setting the rest to zero in (1.1). This class of models should describe the properties of the critical lines shown in Fig. 13. The spins at each site can now assume only p-discrete angles $\theta_n = 2\pi n/p$, $n = 1, \ldots, p$. The interaction energy between two nearest-neighbor angles $\theta(\vec{r})$ and $\theta(\vec{r}')$ in states n and n' is then

$$V(\theta_n(\vec{r}) - \theta_{n'}(\vec{r}')) = K\{1 - \cos[\theta_n(\vec{r}) - \theta_{n'}(\vec{r}')]\} . \tag{3.23}$$

Although the h_p do appear to iterate to infinity when they perturb an isotropic planar model, the isotropic part of the interaction $V(\theta)$ is also changing with iteration. Consequently, (3.23) should be replaced by

$$V_\infty(\theta_n(\vec{r}) - \theta_{n'}(\vec{r}')), \tag{3.24}$$

this being the limiting function $V(\theta)$ approached as h_p iterates to infinity. The precise limiting function is rather difficult to ascertain numerically, and will in fact depend on the initial temperature variable K. Thus we feel it is reasonable to apply the Migdal transformation to $V(\theta)$ in the form

$$e^{V'(\theta_n)} = \sum_{n'=1}^{P} \exp[2V(\theta_{n'}) + 2V(\theta_n - \theta_{n'})] \tag{3.25}$$

in the expectation that the result $V^*(\theta_n)$ of many iterations of (3.25) will not differ essentially from $V_\infty(\theta_n)$. The coupling K appearing in (3.23) must now be interpreted as an effective coupling approached as h_p goes to infinity, and should not be identified with the "bare" or initial temperature variable.

With these caveats and simplications, it is straightforward to analyze the p-state planar models within the Migdal approximation. The manipulations are very similar to those required for the s-state Potts models described in Ref. 25. We have plotted dT_{eff}/dl for these models in Fig. 14.

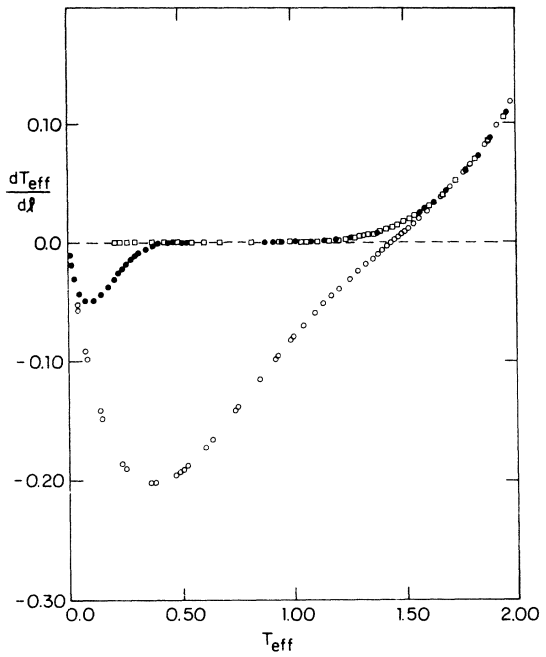

FIG. 14. Differential recursion relations for discrete planar models with $p=6$ (circles) and $p=12$ (dots) states.

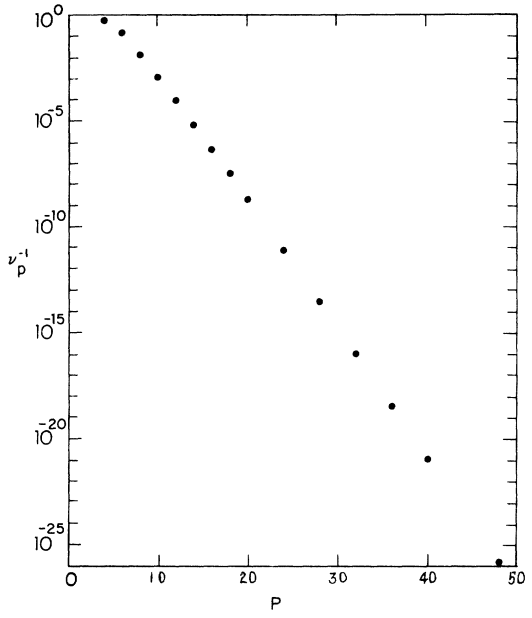

FIG. 15. The critical exponent ν_p^{-1} for a p-state discrete model obtained from the Migdal approximation.

T_{eff} for the discrete models is defined by $V(0) - V(2\pi/p) \equiv 2\pi^2 J/p^2 T_{eff}$, which becomes equivalent to the previous definition (3.9) in the limit $p \to \infty$. All models with $p \geq 2$ appear to have a conventional second-order phase transition at a finite T_c. For $p \geq 8$, dT_{eff}/dl was found to agree closely with the result for the continuous model (Fig. 8) at all temperatures above T_c. Effects of the discreteness of the models were only apparent below T_c. This result is suspect at large p, because it is known that the Migdal transformation fails to predict the first-order character of the transition of s-state Potts models with large s. The critical exponent $\nu(p)$ for these models (which is just the reciprocal of the slope of dT_{eff}/dl through its nontrivial zero) are shown in Fig. 15. As $p \to \infty$, ν diverges, which is not surprising since we should recover an isotropic planar model in this limit.[28] From Fig. 15 we find that $\nu \propto e^{1.0 \cdots}$ for $p \geq 10$.

IV. LATTICE COULOMB GAS AND LOW-TEMPERATURE ANALYSIS

A. Generalized Villain model

We now turn to a more direct and systematic analysis of the low-temperature properties of the planar model. For simplicity we will deal with the Villain model, taking the Fourier-transformed interaction to be

$$\tilde{V}(s) = -s^2/2K_V - \tfrac{1}{2}\ln(2\pi K_V). \tag{4.1}$$

The normalizing constant part of (4.1) is chosen for convenience; we will henceforth drop the subscript on K_V. Recall that the interaction appearing in (1.1) became very similar to the Villain model after a few iterations of the Migdal transformation.

With the choice (4.1), the expression (2.19) for the planar model partition function becomes[29]

$$Z = \sum_{\{m(\vec{R})\}} \left(\prod_{\vec{R}} \int_{-\infty}^{\infty} \frac{d\phi(R)}{2\pi K} \right) \exp\left(\frac{-1}{2K} \sum_{\langle \vec{R}, \vec{R}' \rangle} [\phi(\vec{R}) - \phi(\vec{R}')]^2 + \sum_{\vec{R}} 2\pi i m(\vec{R}) \phi(\vec{R}) \right). \tag{4.2}$$

This exact representation of the partition sum is the result of a dual transformation on the zero-field (all $h_p = 0$) Villain model. Notice that the quadratic coupling term in (4.2) is multiplied by K^{-1}, in contrast to the original problem in which the coupling was proportional to K at low temperatures. This mapping of a strong-coupling problem into a weak-coupling one (and vice versa) is typical of a dual transformation.

For large K, each $\phi(\vec{R})$ in (4.2) undergoes small

fluctuations, and the terms with various $m(\vec{R})$'s different from zero are suppressed. If all the $m(\vec{R})$'s were zero, the mathematics of evaluating (4.2) would be identical to that described in the simple spin-wave analysis of Appendix A. In a limit where finite m excitations can be ignored, we would expect the line of low-temperature fixed points found in spin-wave theory to be essentially correct. However, if the terms with $m(\vec{R})$ nonzero led to important changes in the form of Z, we would expect the spin-wave analysis to be qualitatively incorrect.

To control the size of fluctuations in $m(\vec{R})$, we introduce a new parameter y_0 in Eq. (4.2), writing

$$Z(y_0)=\sum_{\{m(\vec{R})\}}\left(\prod_{\vec{R}}\int_{-\infty}^{\infty}\frac{d\phi(\vec{R})}{2\pi}\right)\exp\left(-\tfrac{1}{2}K\sum_{\langle\vec{R},\vec{R}'\rangle}[\phi(\vec{R})-\phi(\vec{R}')]^2+\sum_{\vec{R}}[\ln y_0 m^2(\vec{R})+2\pi iKm(\vec{R})\phi(\vec{R})]\right). \tag{4.3}$$

We have now converted the part of Z quadratic in $\phi(\vec{R})$ to exactly the spin-wave form of Appendix A by rescaling every $\phi(\vec{R})$ by K. The parameter y_0 controls fluctuations in $m(\vec{R})$. Although our original problem requires $y_0=1$, fluctuations become quite unlikely in the limit $y_0\to 0$. We call the model represented by Eq. (4.3) *the generalized Villain model*.

It is easy to analyze Eq. (4.3) in the limit of small y_0. In this limit, terms with $m_R=0$ dominate, and the terms with $m_R=\pm 1$ can be regarded as a small correction. Thus

$$\begin{aligned}\sum_{m(R)=-\infty}^{\infty}\exp[\ln y_0 m^2(\vec{r})+2\pi iKm(\vec{R})\phi(\vec{R})]&\approx 1+2y_0\cos[2\pi K\phi(\vec{R})]\\&\approx e^{2y_0\cos[2\pi K\phi(\vec{R})]},\end{aligned} \tag{4.4}$$

and (4.3) becomes in the small y_0 limit

$$Z(y_0)=\int d[\phi]\exp\left(-\tfrac{1}{2}K\sum_{\langle\vec{R},\vec{R}'\rangle}[\phi(\vec{R})-\phi(\vec{R}')]^2\right)\times\exp\left(2y_0\sum_{\vec{R}}\cos 2\pi K\phi(\vec{R})\right). \tag{4.5}$$

But this is exactly the spin-wave problem we set for ourselves in Appendix A, in the presence of a "symmetry-breaking field" of the form $\cos(p_{\text{eff}}\theta)$, with

$$p_{\text{eff}}=2\pi K. \tag{4.6}$$

As discussed in Sec. III and in the Appendix, the eigenvalue of such a perturbation is

$$\lambda_{p_{\text{eff}}}(T)=2-p_{\text{eff}}^2/4\pi K=2-\pi K. \tag{4.7}$$

We are lead to the conclusion that finite $m(\vec{R})$ or "vortex" excitations will alter the spin wave results at small y_0 only for

$$K^{-1}=K_B T/J>\tfrac{1}{2}\pi. \tag{4.8}$$

Above this temperature, the y_0 perturbation will break the symmetry. [The neglected terms in the sum (4.4) also produce symmetry-breaking couplings, but these break the symmetry only at temperatures higher than (4.8).] But it is typical of dual models to be in a broken symmetry state when the original problem is in its disordered phase, and vice versa. This information is summarized in the "phase diagram" shown in Fig. 16(a). If we can use some renormalization technique to move from $y_0=0$ to $y_0=1$, we shall know the properties of the Villain model.

B. Reduction to a Coulomb gas

Villain[17] has shown that the model he proposed decomposes exactly into the decoupled spin-wave–vortex system treated by Kosterlitz.[12] We want to show that this representation also follows from the dual transformed Villain model (4.3), as a first step toward a systematic treatment of its low-temperature properties.

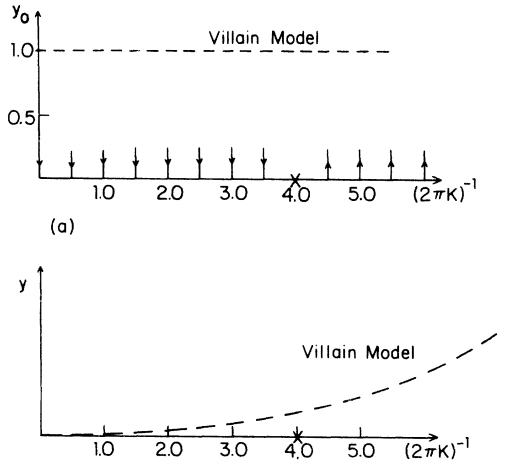

FIG. 16. (a) The Villain model (dashed line) in the space of couplings $2\pi K$ and y_0. As suggested by the arrows, the variable y_0 appears to be an *irrelevant* perturbation to the fixed line at $y_0=0$ for $2\pi K<4$, but is *relevant* for $2\pi K>4$. (b) The Villain model (dashed line) in the space of couplings $2\pi K$ and y. In this representation, the Villain model comes exponentially close to the spin-wave-theory fixed line at low temperatures.

The spin-wave variables $\phi(\vec{R})$ may be eliminated entirely from (4.3) by the usual techniques of Gaussian integration. The result is

$$Z(y_0) = Z_{sw} Z_c(y_0) , \tag{4.9}$$

where Z_{sw} is the spin-wave partition function calculated in Appendix A, and

$$Z_c(y_0) = \sum_{\{m(\vec{R})\}}{}' e^{A_c[m(\vec{R})]} , \tag{4.10}$$

with

$$A_c[m(\vec{R})] = \sum_{\vec{R}} m_R^2 \ln y_0 + \sum_{\text{pairs}} 2\pi K m(\vec{R}) G'(\vec{R} - \vec{R}') m(\vec{R}') . \tag{4.11}$$

The symbol $\sum'$ in (4.10) is a sum over sets of $m(\vec{R})$ such that

$$\sum_{\vec{R}} m(\vec{R}) = 0 , \tag{4.12}$$

while $G'(\vec{R} - \vec{R}')$ is a spin-wave lattice Green's function with a subtraction, defined in Appendix A. The sum over pairs in Eq. (4.11) counts each pair with $\vec{R} \neq \vec{R}'$ exactly once.

Following Kosterlitz and Thouless,[10] we observe that $G'(\vec{R})$ is given to quite a good approximation by[30]

$$G'(\vec{R}) \simeq \ln(R/a_0) + \tfrac{1}{2} \ln(8e^{2\gamma}) \tag{4.13a}$$

for all R, where γ is Euler's constant and a_0 is the lattice space of a square lattice. Alternatively, we could approximate $G'(\vec{R})$ by

$$G'(\vec{R}) \simeq \ln(R/a_0) + \tfrac{1}{2}\pi , \tag{4.13b}$$

which is exact at $R = a_0$ and off by a small additive constant as $R \to \infty$. On inserting either (4.13a) or (4.13b) into (4.11), the partition function (4.10) becomes equivalent to the partition function for a two-dimensional Coulomb gas, with action

$$A_c'[m(\vec{R})] = \sum_{\vec{R}} m^2(\vec{R}) \ln y + \sum_{\text{pairs}} (2\pi K)^{1/2} m(\vec{R}) \ln(|\vec{R} - \vec{R}'|/a_0) \times (2\pi K)^{1/2} m(\vec{R}') . \tag{4.14}$$

The charges are $(2\pi K)^{1/2} \times (0, \pm 1, \pm 2, \ldots)$ and the chemical potential for the production of a charge at a site is

$$y = y_0 e^{-\pi \ln(8e^{2\gamma})K/2} \tag{4.15a}$$

or

$$y = y_0 e^{-\pi^2 K/2} , \tag{4.15b}$$

depending on whether approximation (4.13a) or (4.13b) is used.

Clearly, the parameter y plays the role that y_0 played in our discussion of corrections to spin-wave theory in Sec. IV A. As y tends to zero, the Coulomb partition function Z_c goes to unity and we recover the spin wave results. Figure 16(a) can be redrawn in terms of y as Fig. 16(b), where the Villain model [as defined by (4.14)] becomes exponentially close to a simple spin wave theory at low temperatures.

For future reference, it is useful to display the vortex-vortex correlation which follows from (4.14) in the limit $y \to 0$. Because the dominant non-zero configuration in this limit consists of single excited vortex pair, we find, for $R \neq 0$,

$$\langle m(\vec{0}) m(\vec{R}) \rangle = -2 y_0^2 e^{-2\pi K G'(\vec{R})} \simeq -2 y^2/(R/a_0)^{2\pi K} \quad \text{(large } R\text{)} . \tag{4.16a}$$

When $\vec{R} = \vec{0}$, we find

$$\langle m^2(\vec{0}) \rangle = 2y_0^2 \sum_{\vec{R}} e^{-2\pi K G'(\vec{R})} \simeq 2y^2 \sum_{\vec{R}} \left(\frac{R}{a_0}\right)^{-2\pi K} . \tag{4.16b}$$

Physically, $m(\vec{R})$ represents the quantum number of vortex. Equations (4.16) express the fact that a pair of oppositely oriented vortices can appear in the system with a probability proportional to y^2. They are attracted to each other with a logarithmic potential of strength $2\pi K$.

We are now in a position to develop a sort of "low-temperature series expansion" for the Villain model. To produce a low-temperature series for the *Ising* model in two or three dimensions, one first imagines a configuration of totally up or down spins. Corrections to this dominant configuration at low temperatures are calculated by overturning $1, 2, 3, \ldots$ spins at a time.[31] Here, we expand about an ensemble of states taken into account by a simple spin-wave analysis. Corrections which form a power series in y correspond to the various possible vortex excitations. These ideas will be made explicit by the cumulant expansion described in Sec. IV D.

C. Correlation functions

Before developing a low-temperature cumulant expansion, we describe how to express the correlation function $g_p(\vec{r} - \vec{r}')$ between $e^{ip\theta(\vec{r})}$ and $e^{-ip\theta(\vec{r}')}$ in the Coulomb gas language. According to Eqs. (2.26) and (4.1), the relevant correlation in the Villain model is

$$g_p(\vec{r}-\vec{r}') = Z^{-1}\Big(\sum_{\{m(\vec{R})\}}\prod_{\vec{R}}\int_{-\infty}^{+\infty}\frac{d\phi(\vec{R})}{2\pi K}\Big)\exp\Big(2\pi i\sum_{\vec{R}} m(\vec{R})\phi(\vec{R}) - \frac{1}{2K}\sum_{\langle\vec{R},\vec{R}'\rangle}[\phi(\vec{R})-\phi(\vec{R}')-\eta_{\vec{R},\vec{R}'}p]^2\Big)\,, \quad (4.17)$$

where we remind the reader that the projector operators $\eta_{\vec{R}\vec{R}'}$ are only nonzero on bonds in the dual lattice which cross a previously chosen path from sites $\vec{r}$ to $\vec{r}'$. It is convenient to rewrite (4.17) in terms of new functions $\eta^l(\vec{R})$ and $\eta^r(\vec{R})$:

$$g_p(\vec{r}-\vec{r}') = Z^{-1}\sum_{\vec{R}}\int_{-\infty}^{\infty}\Big(\frac{d\phi(\vec{R})}{2\pi K}\Big)\sum_{\{m(\vec{R})\}}\exp\Big(2\pi i\sum_{\vec{R}} m(\vec{R})\phi(\vec{R}) - \frac{1}{2K}\sum_{\langle\vec{R},\vec{R}'\rangle}[\phi(\vec{R})-\phi(\vec{R}')]^2$$
$$-\frac{p^2}{2K}\sum_{\vec{R}}\eta^2_{\vec{R}\vec{R}} + \frac{p}{K}\sum_{\vec{R}}\phi(R)[\eta^l(\vec{R})-\eta^r(\vec{R})]\Big)\,. \quad (4.18)$$

Here, $\eta^l(\vec{R})$ is a function which is ± 1 at all points on the *left*-hand vertex of a bond which crosses the path from left to right and zero everywhere else: $\eta^r(\vec{R})$ equals unity on the right-hand edge of these bonds and is zero everywhere else (see Fig. 17).

The next to last term in (4.18) counts the number of dual lattice bonds crossed by the path. The mysterious functions $\eta^l(\vec{R})$ and $\eta^r(\vec{R})$ in the final term just give rise to the lattice version of the line integral along the path of the derivative of $\phi(\vec{R})$ perpendicular to that path.

As in the case of the partition function, the integral over the $\phi(\vec{R})$ is easily calculated, with the result

$$g_p(\vec{r}-\vec{r}') = g_p^{sw}(\vec{r}-\vec{r}')g_p^{v}(\vec{r}-\vec{r}')\,. \quad (4.19)$$

The "spin wave" contribution to g_p is

$$g_p^{sw}(\vec{r}-\vec{r}') = \exp-(p^2/2K)X(\vec{r}-\vec{r}')\,, \quad (4.20)$$

where

$$X(\vec{r}-\vec{r}') = \sum_{\vec{R}}\eta^2_{\vec{R},\vec{R}'} - \sum_{\vec{R},\vec{R}'}[\eta^l(\vec{R})-\eta^r(\vec{R})]G(\vec{R}-\vec{R}')$$
$$\times[\eta^l(\vec{R}')-\eta^r(\vec{R}')]\,. \quad (4.21)$$

The vortex contribution is

$$g_p^{v}(\vec{r}-\vec{r}') = \Big\langle\exp\Big(i\sum_{\vec{R}} m(\vec{R})u(\vec{R})\Big)\Big\rangle\,, \quad (4.22)$$

where the expectation is to be calculated in the vortex ensemble (4.11), and

$$u(\vec{R}) = \sum_{\vec{R}'}G'(\vec{R}-\vec{R}')[\eta^l(\vec{R}')-\eta^r(\vec{R}')]\,. \quad (4.23)$$

Although the expression (4.21) entering the "spin wave" part of g_p looks rather formidable, it is shown in Appendix C that (4.21) and (4.20) combine to give the standard spin-wave result (A5):

$$g_p^{sw}(r) = \exp[-(p^2/2\pi K)G'(r)]\,. \quad (4.24)$$

The vortex contribution is, of course, not so simple. However, if $|\vec{r}-\vec{R}|$ and $|\vec{r}'-\vec{R}|$ are large compared to a lattice constant, it can be shown (see Appendix C) that

$$u(\vec{R}) = \Theta(\vec{r}-\vec{R}) - \Theta(\vec{r}'-\vec{R})\,, \quad (4.25)$$

where $\Theta(\vec{r})$ is the shift in orientation of $\Theta(\vec{r})$ produced by a vortex at $\vec{R}=0$:

$$\Theta(r) = \tan^{-1}(y/x)\,,\quad \vec{r}=(x,y)\,. \quad (4.26)$$

Note that if a single uncompensated vortex appears within a distance of order $|\vec{r}-\vec{r}'|$ or $\vec{r}$ and $\vec{r}'$, $u(\vec{R})$ will change by roughly π. As $|\vec{r}-\vec{r}'| \to \infty$, the probability of "destructive interference" of this sort increases, and the correlation function will tend to zero.

D. Fluctuation corrections to the correlations

As an example of the sort of low-temperature expansion possible within this reformulation of the planar model, we calculate the vortex correlation (4.22) to lowest nontrivial order. If the major contribution to (4.22) comes from pairs which are tightly bound, fluctuations in $\sum_{\vec{R}} m(\vec{R})u(\vec{R})$ will be rather small. Consequently, we employ a cummulant expansion, which gives to lowest order

$$g_p^{v}(\vec{r}-\vec{r}') \simeq \exp\Big(-\tfrac{1}{2}p^2\sum_{\vec{R},\vec{R}'}\langle m(\vec{R})m(\vec{R}')\rangle$$
$$\times u(\vec{R})u(\vec{R}')\Big)\,. \quad (4.27)$$

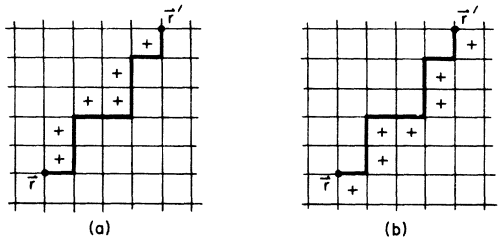

FIG. 17. Definition of the functions $\eta^l(\vec{R})$ and $\eta^r(\vec{R})$ for a particular path. The function $\eta^l(\vec{R})$ is +1 on dual lattice points marked by a cross in lattice (a), and is zero everywhere else. Similarly, $\eta^r(\vec{R})$ is nonzero only on the crosses shown in lattice (b).

To evaluate the sum in (4.27), take $\vec{R}' = \vec{R}_0 + \frac{1}{2}\vec{r}_0 a_0$, $\vec{R} = \vec{R}_0 - \frac{1}{2}\vec{r}_0 a_0$, and assume that $a_0\vec{r}_0$ is small compared to $|\vec{R}_0 - \vec{r}|$ and $|\vec{R}_0 - \vec{r}'|$. This amounts to the assumption that tightly bound vortices dominate the sum for large r and r'. Expanding each $u(\vec{R})$ about $\vec{R}_0$, and making use of the charge neutrality condition $\sum_{\vec{R}} m(\vec{R}) = 0$, we obtain

$$\ln g_p^V(\vec{r} - \vec{r}') = +\tfrac{1}{8} p^2 \sum_{\vec{R}_0, \vec{r}_0} \langle m(\vec{0}) m(a_0\vec{r}_0)\rangle \times a_0^2 [(\vec{r}_0 \cdot \nabla_{\vec{R}_0}) u(\vec{R})]^2 . \quad (4.28)$$

But it follows from (4.25) and (4.26) that

$$\frac{\partial}{\partial x} u(\vec{R}) = \frac{y - Y}{|\vec{r} - \vec{R}|^2} - \frac{y' - Y}{|\vec{r}' - \vec{R}|^2} , \quad (4.29a)$$

$$\frac{\partial}{\partial y} u(\vec{R}) = \frac{x - X}{|\vec{r} - \vec{R}|^2} - \frac{x - X}{|\vec{r}' - \vec{R}'|^2} \quad (4.29b)$$

in this limit. Upon averaging over various orientations, (4.28) can be rewritten

$$\ln g_p^V(\vec{r} - \vec{r}') = \tfrac{1}{16} p^2 \sum \langle m(\vec{0}) m(a_0\vec{r}_0)\rangle a_0^2 r_0^2 \sum_{\vec{R}_0} \nabla_{\vec{R}_0}[G'(\vec{R}_0 - \vec{r}) - G'(\vec{R}_0 - \vec{r}')] \nabla_{\vec{R}_0}[G'(R_0 - \vec{r}) - G'(\vec{R}_0 - \vec{r}')] . \quad (4.30)$$

We can evaluate the sum over R_0 immediately by integrating by parts and observing that

$$\nabla^2 G'(\vec{R}) = -2\pi \delta_{\vec{R},0}/a_0^2 . \quad (4.31)$$

Our result is then that

$$g_p^V(r) = \exp\left(-\tfrac{1}{4}\pi p^2 G'(r) \sum_{\vec{r}_0} r_0^2 \langle m(\vec{0}) m(a_0\vec{r}_0)\rangle\right) . \quad (4.32)$$

This result for the vortex part of the correlation can be combined with the spin-wave contribution (4.24) to give finally

$$g_p(r) = e^{-p^2 G'(r)/2\pi K_{\text{eff}}} , \quad (4.33)$$

where

$$K_{\text{eff}}^{-1} = K^{-1} - \tfrac{1}{2}\pi^2 \sum_{\vec{r}_0} r_0^2 \langle m(\vec{0}) m(a_0\vec{r}_0)\rangle . \quad (4.34)$$

Apparently, the fluctuations in $m(\vec{R})$ have produced a renormalization of K just as in the Migdal approximation of Sec. III. However, the nature of the renormalization is entirely different.

To see this let us look at the contributions from different ranges of $\vec{r}_0$. The low-order calculation described at the end of Sec. IV B gave

$$\langle m(\vec{0}) m(a_0\vec{r}_0)\rangle = -2y^2 e^{-2\pi K G'(a_0\vec{r}_0)} . \quad (4.35)$$

Thus the nearest-neighbor part of (4.34) just gives a contribution to $K_{\text{eff}}^{-1} - K^{-1}$, which is

$$4\pi^2 y^2 e^{-\pi^2 K} . \quad (4.36)$$

However, other ranges of r_0 contribute with quite different weights. In fact, the contribution from higher range of r_0 takes the form

$$\sim \int_{a_0}^{\infty} dr_0 r_0^{3-2\pi K} . \quad (4.37)$$

In the Migdal approximation, all ranges of $\ln r_0$ contribute equally, in contrast to (4.37). Hence, it is inevitable that $K_{\text{eff}} \to 0$ after many interactions. From (4.37) we see that K_{eff} approaches a finite nonzero limit provided

$$2\pi K > 4 . \quad (4.38)$$

The contribution from $r_0 \gtrsim a_0$ dominates in this case.

V. RECURSION RELATIONS AND DUALITY

A. Isotropic recursion relations

Our results and conclusions can be usefully summarized in terms of recursion relations, which are readily derived from the results of Sec. IV. Equation (4.34) for the effective coupling can be turned into a lattice integral equation by noting that, in an improved self-consistent theory, it is K_{eff} and not K which should enter the expression (4.35) for $\langle m(\vec{0}) m(a_0\vec{r}_0)\rangle$. In an approximate continuum form, this integral equation takes the form[32]

$$K_{\text{eff}}^{-1} = K^{-1} + 2\pi^3 y^2 \int_{a_0}^{\infty} \frac{dr}{a_0}\left(\frac{r}{a_0}\right)^{3-2\pi K_{\text{eff}}} . \quad (5.1)$$

For $K_{\text{eff}} < 2/\pi$, the integral diverges and our theory breaks down. To study this further, write out the perturbation series obtained by solving (5.1) iteratively,

$$K_{\text{eff}}^{-1} = K^{-1} + 2\pi^3 y^2 \int_{a_0}^{\infty} \frac{dr}{a_0}\left(\frac{r}{a_0}\right)^{3-2\pi K} + \cdots . \quad (5.2)$$

Now divide each integral into two parts,

$$\int_{a_0}^{\infty} dr = \int_{a_0}^{ba_0} dr + \int_{ba_0}^{\infty} dr , \quad (5.3)$$

with $0 < \ln b \ll 1$. One can combine the small-r parts of the integrals into a new bare coupling

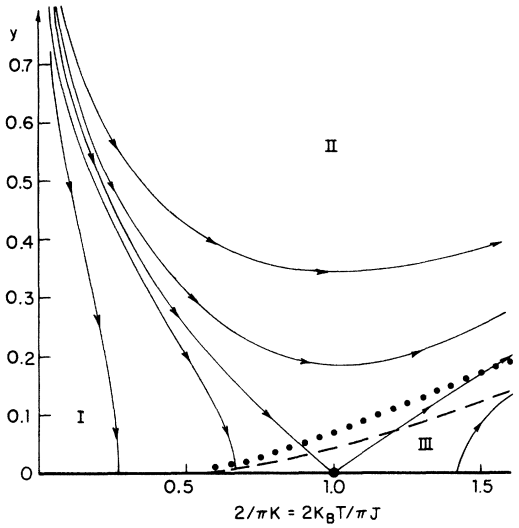

FIG. 18. Renormalization trajectories for the planar model at low temperatures. Two separatrices, which flow in and out of a fixed line at $y=0$, divide the parameter space into three regions.

$(K^{-1})'$, and rescale the large-r integration variables so that the integrals again run from a_0 to ∞. In the limit of small $\ln b$, the integral displayed in (5.2) makes the dominant contribution to $(K^{-1})'$. The rescalings can be absorbed into a redefinition of y.

On resumming the series obtained in this way, one obtains a new integral equation of precisely the same form:

$$K_{\text{eff}}^{-1} = (K^{-1})' + 2\pi^3 y'^2 \int_{a_0}^{\infty} \frac{dr}{a_0}\left(\frac{r}{a_0}\right)^{3-2\pi K_{\text{eff}}}, \tag{5.4}$$

where

$$\begin{aligned}(K^{-1})' &= K^{-1} + 2\pi^3 y^2 \ln b\,,\\ y' &= b^{2-\pi K} y \simeq y + (2-\pi K) y \ln b\,.\end{aligned} \tag{5.5}$$

Apparently, elimination of the short-wavelength part of the integral equation has produced a Coulomb gas problem with parameters $(K^{-1})'$ and y'. A continuous family of such problems is obtained by iterating this transformation. The differential changes in K^{-1} and y are given by

$$\frac{dK^{-1}}{dl} = 2\pi^3 y^2\,, \tag{5.6a}$$

$$\frac{dy}{dl} = (2-\pi K) y\,, \tag{5.6b}$$

where $l = \ln b$. Except for minor differences, these are precisely the equations obtained previously by Kosterlitz.[12]

Figure 18 shows the renormalization trajectories obtained from (5.6) (this is a low-temperature version of Kosterlitz's Fig. 1). The spin-wave theory fixed line of Berezinskii is given by $y=0$. The parameter space divides into three regions, partitioned by two separating lines (separatrices) which lead in and out of the fixed line. The fixed line is *stable* to vortex perturbations in region I, as was suggested by the arguments of Sec. IV A. Actions initially in regions II and III iterate toward large y, outside the range of our small-y theory. The locus of initial Hamiltonians for the Villain model is shown by the dashed curve in Fig. 18. Formula (4.33) for $g_p(r)$ applies to the Villain model only when it is in region I.

It is tempting to associate T_c with the intersection of the Villain locus and the left-hand separatrix of Fig. 18 as was done by Kosterlitz.[12] Certainly, a very plausible assumption is that both regions II and III ultimately flow into a high-temperature fixed point. Under this assumption, Kosterlitz showed that the correlation length, infinite below T_c, diverges as

$$\xi(T) \sim e^{\text{const}/|T-T_c|^{1/2}}, \tag{5.7}$$

as $T \to T_c$ from above.[33] A second consequence[12] is that the critical exponent η obtains a universal value

$$\eta = \tfrac{1}{4} \tag{5.8}$$

at T_c.

Unfortunately, Luther and Scalapino's recent solution of a planar model[13] casts doubt on this simple picture. Their calculations suggest that the value of η at T_c is nonuniversal, depending on the details of the particular planar model. This would require another marginal operator (in addition to K^{-1}) in the theory. The only such operators we have found (other than trivial ones) are associated with symmetry-breaking fields.

However, there is one way out. We showed in Sec. IV A that the leading vortex perturbations to spin-wave theory could be viewed as a symmetry-breaking operator $\cos(p_{\text{eff}}\phi)$ with $p_{\text{eff}} = 2\pi K$.[34] The vortex perturbations become relevant at precisely $p_{\text{eff}} = 4$. One might speculate that, for large y in region II, the model goes over into a system with an infinitely strong symmetry-breaking field with $p_{\text{eff}} \simeq 4$. It is not difficult to show that this would be an Ashkin-Teller model. The planar model could possibly have the continuously variable exponents of spin-wave theory in region I, the exponents of the Ashkin-Teller model in region II, and a high-temperature phase only in region III. Conceivably, this could happen in a way consistent with the Luther-Scalapino results.

In region I, where the physics is presumably well understood, it is of interest to calculate the eigenvalues of various symmetry-breaking fields.

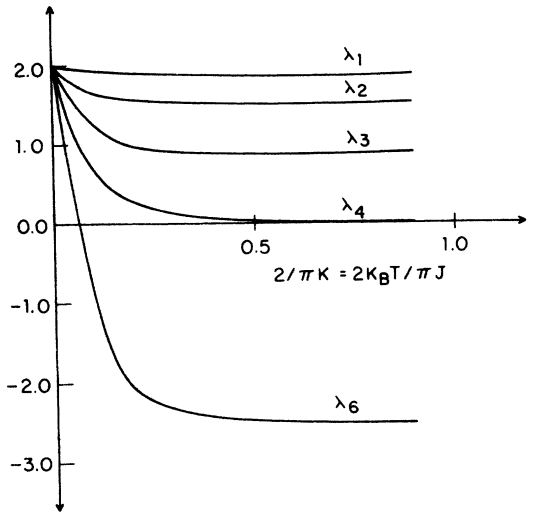

FIG. 19. Eigenvalues $\lambda_p(T)$ for symmetry-breaking fields applied to the Villain model obtained by taking vortex corrections to spin-wave theory. We cannot calculate the $\lambda_p(T)$ beyond $2k_BT\pi J = 0.9$, which may actually correspond to the critical temperature of the model.

This was done by Kosterlitz only for $p = 1$. From Fig. 1, we see that these eigenvalues are determined simply by the mapping (5.6) of the Villain model onto spin-wave theory. According to (4.33),

$$g_p(r) \sim 1/r^{\eta_p(T)}, \quad \eta_p(T) = p^2/2\pi K_{\text{eff}}, \tag{5.9}$$

at large r. Because (see Appendix A)

$$\lambda_p(T) = 2 - \tfrac{1}{2}\eta_p(T), \tag{5.10}$$

$\lambda_p(T)$ follows from an approximate calculation of K_{eff}. These eigenvalues are shown in Fig. 19. They are calculable within this approach only up to the border of region II, where $2k_BT/\pi J \simeq 0.9$. Each $\lambda_p(T)$ varies smoothly from 2 to $2 - \frac{1}{8}p^2$. The important point is that $\lambda_6(T)$ goes negative at sufficiently high temperatures, above which h_6 is irrelevant. Above this temperature (but below the Kosterlitz-Thouless T_c), planar model behavior should be experimentally accessible in quasi-two-dimensional crystals dominated by hexagonal anisotropies. The eigenvalue $\lambda_4(T)$ goes to zero at precisely the transition temperature marking the border of regions I and II. In Sec. V C we show that cubic perturbations, which are *marginal* at this apparent T_c, actually sweep out a new (Baxter-like) line of fixed points. The critical behavior (if any) when the $\lambda_p(T)$ are relevant is impossible to ascertain except within the untrustworthy Migdal approach of Sec. III. Comparing Fig. 19 with the results displayed in Fig. 12, we see that the Migdal results may not be too bad for $p = 1$–3.

B. Duality results

To proceed further, we quote a duality result which is proved in Appendix D. So far, we have considered the partition function of the Villain model with coupling K, and an extra parameter y_0 introduced into the dual model in Eq. (4.3). In addition, we have been interested in the effects of field terms, expressed as contributions to the exponentiated action of the form given in Eq. (1.1)

$$\prod_r e^{h_p \cos[p\theta(r)]} = \Lambda. \tag{5.11a}$$

It is only a small change to replace Λ by

$$\Lambda' = \prod_r \sum_{\{n(r)\}} \exp\{ip\theta(r)n(r) + \ln y_p[n(r)]^2\}. \tag{5.11b}$$

If $y_p \to 0$, only the terms $n = 0$ and ± 1 contribute, and Λ' goes into Λ provided

$$h_p = \tfrac{1}{2}y_p. \tag{5.12}$$

If $y_p \to 1$, then $\theta(r)$ is forced to take on the values

$$(2\pi/p)q(r); \quad q(r) = 0, 1, 2, \ldots, p-1,$$

appropriate to the p-state model. Hence $y_p \to 1$ is just like $h_p \to \infty$.

Imagine a problem which contains in the $\theta(r)$ picture a term like $\ln\Lambda'$ in its action and is otherwise identical to our generalized Villain model. This problem is defined more explicitly in Appendix D. There it is proven that the partition function of this model $Z(2\pi K, y_0, y_p)$ obeys the duality relation

$$Z(2\pi K, y_0, y_p) = Z(p^2/2\pi K, y_p, y_0)(p/2\pi K)^N. \tag{5.13}$$

We know that the generalized Villain model has a Kosterlitz-Thouless critical point at

$$2\pi K \simeq 4, \tag{5.14a}$$

as $y_0 \to 0$ and $y_p \to 0$. Equation (5.13) then directly implies that this model also has another singularity at

$$2\pi K \simeq \tfrac{1}{4}p^2, \tag{5.14b}$$

in the presence of a small-h_p (or y_p) type perturbation. And the singularities in the free energy must be identical! The transition (5.14b) is the change from behavior characteristic of the p-state model to planar model behavior. Thus the duality relation maps all these p-state to planar transitions into the Kosterlitz-Thouless "point." Since an infinite number of different transitions map into this "point," we have at least suggestive evidence that this "point" contains quite a bit of structure. It could conceivably represent a whole family of different universality classes, which would be consistent with the Luther-Scalapino picture.

For $y_0 = y_p = 1$, we have a p-state version of the Villain model. Villain[17] estimated that a phase transition at $p = \infty$ took place when

$$K \simeq 1/1.7 .$$

Hence for large p, we expect the transition from the p-state Villain model to the planar behavior to occur at

$$K \simeq [p^2/(2\pi)^2]1.7 .$$

We expect this transition to occur provided $p \geq 4$.

C. Recursion relations with symmetry-breaking fields

The duality relation quoted in Sec. V B can be used to generalize Eqs. (5.6) to allow for symmetry-breaking fields. Setting $y = y_0 e^{-(1/2)\pi^2 K}$, we can rewrite (5.6) in the form

$$\frac{dK^{-1}}{dl} = 2\pi^3 y_0^2 e^{-\pi^2 K} , \tag{5.15a}$$

$$\frac{dy_0}{dl} = (2 - \pi K) y_0 , \tag{5.15b}$$

where these equations are correct to leading order in y_0. By exploiting the duality relation (5.13) with $y_p = 0$, these equations can be used to produce recursion relations for K^{-1} and y_p with $y_0 = 0$,

$$\frac{dK^{-1}}{dl} = -\tfrac{1}{2}\pi p^2 y_p^2 K^{-2} e^{-p^2 K^{-1}/4} , \tag{5.16a}$$

$$\frac{dy_p}{dl} = \left(2 - \frac{p^2}{4\pi} K^{-1}\right) y_p , \tag{5.16b}$$

correct to lowest order in y_p.

It is tempting to combine (5.15) and (5.16) into a set of recursion relations which might be valid for both y_p and y_0 nonzero:

$$\frac{dK^{-1}}{dl} = 2\pi^3 y_0^2 e^{-\pi^2 K} - \tfrac{1}{2}\pi p^2 y_p^2 K^{-2} e^{-p^2 K^{-1}/4} , \tag{5.17a}$$

$$\frac{dy_0}{dl} = (2 - \pi K) y_0 , \tag{5.17b}$$

$$\frac{dy_p}{dl} = \left(2 - \frac{p^2}{4\pi} K^{-1}\right) y_p . \tag{5.17c}$$

By construction Eqs. (5.17) obey the duality relation (5.13) and reduce to the correct limits when either y_0 or y_p tends to zero. Furthermore, no additional terms can appear in (5.17) to lowest order in y_0 and y_p by symmetry. For example, a term proportional to $y_0 y_p$ cannot appear in (5.17a) because the equations must be invariant under $y_p \to -y_p$. Similarly, terms proportional to y_p or y_p^2 cannot appear into (5.17b): duality would demand y_0 and y_0^2 terms in (5.17c), again violating invariance under $y_p \to -y_p$. We are led to the conclusion that Eqs. (5.17) are correct as they stand to lowest order in y_0 and y_p.

The differential equations (5.17) give strong evidence for the phase diagram in Fig. 1(a) for $p > 4$. As the initial temperature is varied for fixed $h_p = \frac{1}{2} y_p \neq 0$, we find from (5.17) that a segment of the Berezinskii fixed line is stable to both vortex and h_p perturbations. The vortex parameter y_0 becomes unstable and iterates toward large values for $T > T_1(h_p)$, while h_p becomes unstable and iterates toward large values for $T < T_2(h_p)$. We are led immediately to a phase diagram like that in Fig. 1(a), provided we associate the instability for $T > T_1(h_p)$ with a disordered phase, and the instability for $T < T_2(h_p)$ with an ordered p-state phase.

The critical properties for small y_0 and y_p with $p = 4$ are controlled by *three* fixed lines. In addition to the Berezinskii spin-wave fixed line ($y_4 = y_0 = 0$, K^{-1} arbitrary), we find two new fixed lines in (5.17) given by

$$K^{-1} = \tfrac{1}{2}\pi , \quad y_0 = \pm y_4 . \tag{5.18}$$

Every point with $y_0 = \pm y_4 \neq 0$ along these lines is characterized by one marginal, one irrelevant, and one relevant eigenvalue. The two new fixed lines have two-dimensional domains of attraction in the $(K^{-1}\text{-}y_0\text{-}y_4)$-Hamiltonian space, and control the critical behavior for $y_4 \neq 0$. It is straightforward to show that this description in terms of three fixed lines leads to the phase diagram shown in Fig. 1(b). All three lines display continuously variable critical exponents with a conventional phase transition across $T_c(h_4)$.[35] Although the exponent $\eta(h_4)$ remains fixed at $\frac{1}{4}$ to lowest order in h_4, we find that the correlation length exponent $\nu(h_4)$ diverges,

$$\nu(h_4) \sim 1/|h_4| ,$$

as $h_4 \to 0$.

For $p < 4$ the entire spin-wave fixed line is unstable to either vortex or h_p perturbations, and we are unable to determine the critical behavior for small $h_p \neq 0$. Presumably, two Ising (Potts) critical lines are present in the $(h_p\text{-}T)$ plane for $p = 2$ ($p = 3$). Further investigation is required to determine how these lines connect up to the phase diagram of the planar model for $h_p = 0$.

ACKNOWLEDGMENTS

We were helped by stimulating conversations with M. Fisher, B. I. Halperin, A. Luther, P. C. Martin, and E. Witten. We are grateful in addition for an informative correspondence with J. M. Kosterlitz.

APPENDIX A: SPIN-WAVE THEORY

In this appendix we review the standard source of low-temperature results for models with contin-

uous symmetry, spin-wave theory. The usual route to this approximation is to expand the interaction function in (1.1) to second order in $\theta(\vec{r}) - \theta(\vec{r}')$, so that it takes the form

$$A[\theta] - \tfrac{1}{2}K \sum_{\langle \vec{r}, \vec{r}' \rangle} [\theta(\vec{r}) - \theta(\vec{r}')]^2 + \sum_{\vec{r}, p} h_p \cos[p\theta(\vec{r})] . \tag{A1}$$

Then, the variables $\theta(\vec{r})$ (which can be chosen to take on values in the region $[-\pi, \pi]$) are replaced by variables $\phi(\vec{r})$ which run over all real values.[7,8] In Sec. IV, it is shown that the dual representation of the Villain models involves an action of precisely this form. In the $h_p \to 0$ limit, all properties of the resulting Gaussian action can be evaluated quite explicitly.

As an approximation to (1.1), the spin-wave results are expected to be valid in the low-temperature limit. Neglected terms of order $K[\theta(\vec{r}) - \theta(\vec{r}')]^n$, $n = 4, 6, \ldots$, produce interactions between spin waves and corrections of relative order K^{-1}. The extension of the range of integration to $\pm\infty$ eliminates vortex excitations, which are of relative order $e^{-\pi^2 K}$.[36,37]

The action which produces the spin wave approximation can be written in the form

$$A[\phi] = -\tfrac{1}{2}K \sum_{\langle \vec{r}, \vec{r}' \rangle} \phi(\vec{r}) G^{-1}(\vec{r} - \vec{r}') \phi(r') , \tag{A2}$$

where $G(\vec{r} - \vec{r}')$ is the lattice Green's function derived from (A1) for $h_p = 0$. This Green's function and its inverse may be written

$$G^{\pm 1}(\vec{r}) = \int_{-\pi}^{\pi} \frac{dq_x}{2\pi} \int_{-\pi}^{+\pi} \frac{dq_y}{2\pi} \frac{e^{-i\vec{q}\cdot(\vec{r}-\vec{r}')/a_0}}{(4 - 2\cos q_x - 2\cos q_y)^{\pm 1}} . \tag{A3}$$

Using (A3), it is very easy to produce the spin-wave partition function, which is

$$Z_{sw} = \left(\prod_{\vec{R}} \int_{-\infty}^{+\infty} \frac{d\phi(\vec{R})}{2\pi} \right) e^{A[\phi]} = \exp\left[-\tfrac{1}{2}\Omega \int_{-\pi}^{\pi} \frac{dq_x}{2\pi} \int_{-\pi}^{\pi} \frac{dq_y}{2\pi} \ln\left(\frac{K}{2\pi} (4 - 2\cos q_x - 2\cos q_y) \right) \right] , \tag{A4}$$

where Ω is the size of the system.

More interesting results obtainable within the spin-wave approximation are the correlation functions corresponding to the various h_p perturbations entering (A1). For example, it is straightforward to calculate

$$g_p^{sw}(\vec{r} - \vec{r}') = \langle e^{ip[\theta(\vec{r}) - \theta(\vec{r}')]} \rangle = e^{-(p^2/2\pi K) G'(\vec{r} - \vec{r}')} , \tag{A5}$$

where

$$G'(\vec{r}) = 2\pi[G(0) - G(\vec{r})] . \tag{A6}$$

Note that the infrared singularity in $G(\vec{r})$ produces an asymptotic form for $G'(r)$, which is

$$G'(\vec{r}) = \ln(r/a_0) + \text{const} , \tag{A7}$$

as $r \to \infty$. Thus, the spin-wave correlation function at large separations is

$$G_p^{sw}(\vec{r} - \vec{r}') \sim (|\vec{r} - \vec{r}'|/a_0)^{-p^2/2\pi K} . \tag{A8}$$

In a standard scaling theory of critical phenomena, we would interpret (A8) as a statement that the action (A2) is at a critical point, and that the perturbation $e^{ip\phi(r)}$ {or, equivalently, $\cos[p\phi(\vec{r})]$} had scaling index

$$x_p = p^2/4\pi K. \tag{A9}$$

The corresponding field h_p has a scaling index λ_p, which is $\lambda_p = d - x_p$, where d is the dimensionality. Consequently we have

$$\lambda_p = 2 - p^2/4\pi K . \tag{A10}$$

a result which is discussed in Sec. III C.

APPENDIX B: SYMMETRY-BREAKING FIELDS AND THE MIGDAL APPROXIMATION

The Migdal recursion scheme is fairly ambiguous in its treatment of symmetry-breaking fields. As shown in Fig. 20 one can imagine moving an arbitrary fraction α of the field on each site in the initial bond-moving step. A heuristic argument which suggests what fraction should be moved is summarized graphically in Fig. 21. One divides each on-site field symmetrically between the four connecting bonds, and then manipulates each bond-

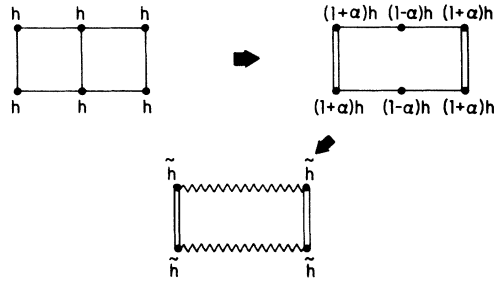

FIG. 20. Potential moving scheme for handling an on-site interaction within the Migdal approximation. The parameter α is, at present, arbitrary.

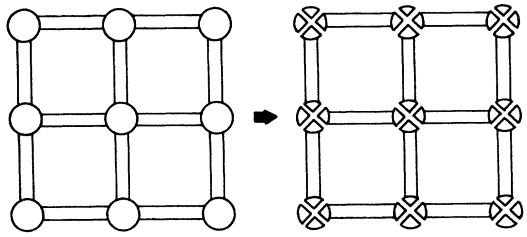

FIG. 21. Scheme for partitioning an onsite potential into four equal parts such that it can be treated by a bond-moving approach. The enlarged vertices represent the on-site potential.

plus-field component as before.[38] On a d-dimensional hypercubical lattice, this would lead to the requirement

$$\alpha = 1/d . \tag{B1}$$

Once α is specified, our procedure for handling symmetry-breaking fields in the Migdal approach is straightforward and well defined. Because of the importance of choosing α properly, we now sketch an alternative argument which produces the results $\alpha = \frac{1}{2}$ in $d = 2$, in agreement with (B1).

It is well known that the Migdal approach[14] gives results for the correlation length exponent ν which agree, to leading order, with the more complicated spin-wave theories[15,16] in $2+\epsilon$ dimensions for n-component isotropic fixed-length spin models. It does, however, produce $T_c(n,\epsilon)$ incorrectly, a quantity which should be *universal* to first order in ϵ.[16] The competing results are, from the spin-wave analysis,

$$k_B T_c(n,\epsilon)/J = 2\pi\epsilon/(n-2) + O(\epsilon^2) , \tag{B2a}$$

and from the Migdal approach,

$$k_B T_c(n,\epsilon)/J = 4\epsilon/(n-2) + O(\epsilon^2) . \tag{B2b}$$

We can define a characteristic temperature scale T_0 for the case of interest here ($n = 2$, $\epsilon = 0$) by taking a limit:

$$\frac{k_B T_0}{J} = \lim_{\epsilon\to 0}\lim_{n\to 2} \frac{(n-2)k_B T_c(n,\epsilon)}{\epsilon J} = \begin{cases} 2\pi \\ 4 \end{cases} . \tag{B3a}$$

The Migdal approximation may be carried out analytically at low temperature on the "spin wave" action of Eq. (A1), with the result

$$\begin{aligned} \lambda_p(T) &= 2 - \tfrac{1}{4}(1-\alpha)p^2 k_B T/J \\ &= 2 - (1-\alpha)p^2(T/T_0) , \end{aligned} \tag{B4}$$

where we have expressed our results in terms of the temperature scale T_0 appropriate to the Migdal approach. The result (A10) from spin-wave theory may be rewritten in the form

$$\lambda_p = 2 - \tfrac{1}{2}p^2(T/T_0) , \tag{B5}$$

where T_0 is determined from the spin-wave result. The requirement that the coefficients of (T/T_0) in these expansions agree suggests that we take

$$\alpha = \tfrac{1}{2} . \tag{B6}$$

The reader may view this particular route to the result $\alpha = \frac{1}{2}$ as somewhat capricious. Similar arguments, however, show that the choice $\alpha = \frac{1}{2}$ is necessary to get the eigenvalues of symmetry-breaking fields[36] correct for $n \geq 3$ and $d = 2+\epsilon$. This choice of α enables the Migdal recursion scheme to get exponents correct, even though it underestimates $T_c(n,\epsilon)$.

APPENDIX C: MANIPULATIONS ON LATTICE PATH INTEGRALS

We wish to evaluate

$$\begin{aligned} X(\vec{r}-\vec{r}') = &\sum_{\vec{R}} \eta^2_{\vec{R},\vec{R}'} \\ &- \sum_{\vec{R},\vec{R}'} [\eta^l(\vec{R}) - \eta^r(\vec{R})]\, G(\vec{r}-\vec{r}') \\ &\times [\eta^l(\vec{R}') - \eta^r(\vec{R}')] . \end{aligned} \tag{C1}$$

The first term just gives the length of the path from $\vec{r}$ to $\vec{r}'$ [see Fig. 17(a)]. The definitions of $\eta^l(\vec{R})$ and $\eta^r(\vec{R}')$ restrict both sums in the second term to be in the neighborhood of this same path. The quantities $[\eta^l(\vec{R}) - \eta^r(\vec{R})]$ and $[\eta^l(\vec{R}') - \eta^r(\vec{R}')]$ are operators acting on $G(\vec{R}-\vec{R}')$ which generate the discrete analog of a perpendicular derivative along the path.

Equation (C1) can be rewritten in a convenient continuum notation

$$X(\vec{r}-\vec{r}') = \int_{\text{path}} dR - \int_{\text{path}} dR \int_{\text{path}} dR'\, \partial_\perp \partial'_\perp G(\vec{R}-\vec{R}') , \tag{C2}$$

where $\partial_\perp$ and $\partial'_\perp$ are perpendicular derivatives with respect to $\vec{R}$ and $\vec{R}'$, respectively. The scalar symbols dR and dR' represent line elements along the path. It is straightforward to transform this continuum notation back into the lattice language. The second term of (C2) can be simplified

$$\begin{aligned} &\int_{\text{path}} dR \int_{\text{path}} dR'\, \partial_\perp \partial'_\perp G(\vec{R}-\vec{R}') \\ &= -\int_{\text{path}} dR \int_{\text{path}} \partial'^2_\perp G(\vec{R}-\vec{R}') \\ &= -\int_{\text{path}} dR \int_{\text{path}} dR' [\nabla^2 G(\vec{R}-\vec{R}') - \partial'^2_{\parallel} G(\vec{R}-\vec{R}')] , \end{aligned} \tag{C3}$$

where $\partial_{\parallel}$ denotes a derivative along the path. Since $\nabla^2 G(\vec{R}-\vec{R}')$ is zero except at $\vec{R} = \vec{R}'$, the first term

of (C3) reduces to the path integral of unity and cancels the first term of (C2). We have finally

$$X(\vec{r}-\vec{r}') = \int_{\text{path}} dR \int_{\text{path}} dR'\, \partial_{\parallel}^2\, G(\vec{R}-\vec{R}')$$
$$= -\int_{\text{path}} dR \int_{\text{path}} dR'\, \partial_{\parallel}\, \partial_{\parallel}'\, G(\vec{R}-\vec{R}')$$
$$= -2[G(\vec{r}_1-\vec{r}_2)-G(0)] = G'(|\vec{r}-\vec{r}'|)/\pi\,, \tag{C4}$$

which gives the desired spin-wave result.

The path integral

$$u(\vec{R}) = \sum_{\vec{R}}\; G'(\vec{R}-\vec{R}')[\eta^l(\vec{R}')-\eta^r(\vec{R}')] \tag{C5}$$

can be handled in much the same way. For large separations $|\vec{R}-\vec{r}'|$ and $|\vec{R}-\vec{r}|$ this can be rewritten (again in continuum notation)

$$u(\vec{R}) = \int_{\text{path}} dR'\, \partial_{\perp}'\ln(|\vec{R}-\vec{R}'|). \tag{C6}$$

Let us regard $\ln(|\vec{R}-\vec{R}'|)$ as the real part of a complex function $\ln(z-z')$, $z = R_x + iR_y'$, $z' = R_x' + iR_y'$, so that

$$\ln(|\vec{R}-\vec{R}'|) = \mathrm{Re}[\ln(z-z')]\,, \tag{C7}$$

and consider the path integral as occurring in the complex z' plane:

$$u(z) = \int_{\text{path}} dz'\, \partial_{\perp}'\, \mathrm{Re}[\ln(z-z')]\,. \tag{C8}$$

This can be evaluated using the Cauchy-Riemann relation

$$u(z) = -\int_{\text{path}} dz'\, \partial_{\parallel}'\, \mathrm{Im}[\ln(z-z')]$$
$$= \Theta(\vec{r}-\vec{R}) - \Theta(\vec{r}'-\vec{R})\,, \tag{C9}$$

where

$$\Theta(\vec{R}) = \tan^{-1}(x/y)\,. \tag{C10}$$

APPENDIX D: GENERALIZED MODELS AND DUALITY

For the sake of completeness and also to make contact with the gauge field literature,[40] we construct a rather general form of the duality relations for our type of model.

Start from our generalized version of the Villain model on the dual lattice, i.e., Eq. (2.19) with the extra $\ln y_0$ term of Eq. (4.3). Hence our expression for the partition function reads

$$Z(2\pi K, y_0, 0) = \sum_{\{\tilde{m}(R)\}} \left(\prod_{\vec{R}} \int_{-\infty}^{\infty} \frac{d\tilde{\phi}(R)}{2\pi K}\right) \exp \tilde{A}[\tilde{\phi}, \tilde{m}]\,, \tag{D1}$$

with

$$\tilde{A}[\tilde{\phi}, \tilde{m}] = -\sum_{\langle \vec{R}, \vec{R}'\rangle} \frac{1}{2K}\,[\tilde{\phi}(\vec{R}) - \tilde{\phi}(\vec{R}')]^2$$
$$+ \sum_{\vec{R}} \{2\pi i\, \tilde{\phi}(R)\tilde{m}(R) + (\ln y_0)[\tilde{m}(\vec{R})]^2\}\,. \tag{D2}$$

For future convenience, in (D1) Z has been written as a function of three variables—one of which is set equal to zero. The "space" is being saved for a symmetry-breaking field, which is being held to zero at this point.

To understand this model, undo the dual transformation. Write $e^{\tilde{v}} \equiv e^{-(1/2K)[\tilde{\phi}(\vec{R})-\tilde{\phi}(\vec{R}')]^2}$ as a Fourier integral

$$e^{\tilde{v}(\tilde{\phi}(R)-\tilde{\phi}(R'))} = \int_{-\infty}^{\infty} \frac{d\phi(\vec{R},\vec{R}')}{2\pi}\; e^{v_0(\phi(\vec{R},\vec{R}'))}$$
$$\times\, e^{i\phi(\vec{R},\vec{R}')[\tilde{\phi}(\vec{R})-\tilde{\phi}(R')]}\,, \tag{D3}$$

and substitute the result in Eq. (D1). Then the $\tilde{\phi}(R)$ integrals can be calculated immediately to yield a result directly analogous to Eq. (2.16), namely

$$Z(2\pi K, y_0, 0) = \sum_{\tilde{m}(R)} \left(\prod_{\langle \vec{R}\vec{R}'\rangle} \int_{-\infty}^{\infty} \frac{d\phi(\vec{R},\vec{R}')}{2\pi}\right) \left(\prod_{\vec{R}} \tilde{\Delta}(\vec{R})\right) \exp\left(-\sum_{\langle \vec{R},\vec{R}'\rangle} \tfrac{1}{2}K[\phi(\vec{R},\vec{R}')]^2 + \sum_{\vec{R}} (\ln y_0)[\tilde{m}(R)]^2\right). \tag{D4}$$

In writing Eq. (D4), we have evaluated the Fourier transform in Eq. (D3). In (D4), $\tilde{\Delta}(R)$ is a δ function essentially similar to the one in Eq. (2.15). In particular, for the arrangement of points shown in Fig. 22,

$$\tilde{\Delta}(R) = 2\pi\delta(\phi(R,R_1) + \phi(R,R_2)$$
$$- \phi(R_1',R) - \phi(R_2',R) + 2\pi\tilde{m}(R))\,. \tag{D5}$$

Just as before, one can "solve" the δ-function conditions (D5) by writing $\phi(R,R')$ in terms of quantities which refer to the dual lattice. In particular, each nearest-neighbor bond on the dual lattice is cut by one and only one bond on the original lattice. Thus, we can relabel each $\phi(R,R')$ as a $\phi(r,r')$. For example, $\phi(R,R_1)$ in Fig. 22 can also be written $\phi(r_1,r_2)$. Given this relabeling we can rewrite the δ function (A6) as

$$\Delta(R) = 2\pi\delta(\phi(r_1,r_2) + \phi(r_4,r_1)$$
$$- \phi(r_4,r_3) - \phi(r_3,r_2) + 2\pi\tilde{m}(R))\,. \tag{D6}$$

This δ-function condition can, in turn be satisfied by

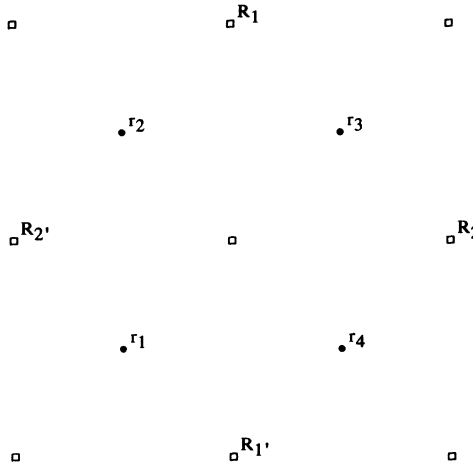

FIG. 22. Dual and original lattice points. Squares represent points of the dual lattice, dots sites in the original lattice.

$$\phi(r_1,r_2)=\theta(r_1)-\theta(r_2)-m(r_1,r_2)\,. \tag{D7}$$

Here, the θ's are required to be in the interval $0<\theta(r)\leq 2\pi$ and the integers $m(r_1,r_2)$ are adjusted to keep the θ's in this range.

One further condition is required. Equation (D6) requires that the sum of the $m(r_1,r_2)$ around the loop, i.e.,

$$S_R(m)=m(r_4,r_1)+m(r_1,r_2)-m(r_3,r_2)-m(r_4,r_3)\,, \tag{D8}$$

be equal to $\vec{m}(R)$. Equations (D7) and (D8) ensure that the δ function conditions are all properly satisfied. Then (D4) is seen to read

$$Z(2\pi K,y_0,0)=\left(\prod_{\vec{r}}\int_0^{2\pi}\frac{d\theta(r)}{2\pi}\right)\sum_{m(r,r')}e^{A[\theta,m]}\,, \tag{D9}$$

where the new action is

$$A[\theta,m]=-\tfrac{1}{2}K\sum_{\langle r,r'\rangle}[\theta(\vec{r})-\theta(\vec{r}')-2\pi m(\vec{r},\vec{r}')]^2+\sum_R(\ln y_0)[S_R(m)]^2\,. \tag{D10}$$

Notice how the periodicity in $\theta(r)$ is reflected in the action (D10). This action is invariant under the "gauge transformation"

$$\theta(\vec{r})\to\theta(\vec{r})+2\pi n(\vec{r})\,,\qquad m(\vec{r},\vec{r}')\to m(\vec{r},\vec{r}')+n(\vec{r})-n(\vec{r}')\,. \tag{D11}$$

[Note that $S_R(m)$ is invariant under (D11).] Hence the result of the summations over m in Eq. (D9) is a completely periodic function of each $\theta(\vec{r})$.

The reason that our analysis gave a very simple $y_0\to 0$ limit can also be seen from these equations. As $y_0\to 0$, the only terms in the m sums which contribute are those with $S_R(m)=0$ for all R. This condition will in turn be satisfied if

$$m(r_1,r_2)=n(r_1)-n(r_2)\,. \tag{D12}$$

Thence, the major contribution to Z as $y_0\to 0$ is

$$\lim_{y_0\to 0}Z(2\pi K,y_0,0)=\prod_r\left(\int_0^{2\pi}\frac{d\theta(r)}{2\pi}\sum_{n(r)}\right)\exp-\sum_{\langle r,r'\rangle}\tfrac{1}{2}K[2\pi\phi(r)-2\pi\phi(r')]^2\,. \tag{D13}$$

where

$$2\pi\phi(r)=\theta(r)-2\pi n(r)\,. \tag{D14}$$

But the sum over $n(r)$ and the integral over $\theta(r)$ combine to give a simple result

$$\int_0^{2\pi}\frac{d\theta(r)}{2\pi}\sum_{n(r)}=\int_{-\infty}^{\infty}d\phi(r)\,.$$

Hence in the limit $y_0\to 0$, all effects of periodicity in $\theta(r)$ completely vanish and we are left with a linear spin-wave problem.

One can also incorporate the symmetry-breaking terms with exactly the same analysis. Recall that the action (1.1) contained terms like

$$\sum_r\sum_p h_p\cos[p\theta(r)]\,.$$

But, by suitably choosing a function $f_p(n)$ we can always adjust a sum of the form

$$\sum_n e^{(\ln y_p)f_p(n)+i\theta np} \tag{D15}$$

to be an exponential like

$$e^{h_p\cos p\theta}\,. \tag{D16}$$

For example, let us choose h_p to be very small, $h_p\ll 1$. Then take

$$y_p=\tfrac{1}{2}h_p\ll 1$$

and

$$f_p(n)=n^2\,. \tag{D17}$$

With these choices (D15) and (D16) agree to first order in y_p.

Furthermore, if one chooses $y_p\to 1$, then the sum (D15) vanishes unless θ takes on one of the

values appropriate to the p-state model. In this case, expression (D15) reduces to

$$\sum_{q=0}^{p-1} \delta\left(\frac{\theta}{2\pi} - \frac{q}{p}\right). \tag{D18}$$

In short (D15) can represent symmetry-breaking fields as $y_p \to 0$ and the p-state model as $y_p \to 1$.

For this reason, we consider the generalization of Eq. (D9) which reads

$$Z(2\pi K, y_0, y_p) = \left(\prod_{\vec{r}} \int_0^{2\pi} \frac{d\theta(\vec{r})}{2\pi}\right) \sum_{\{m(\vec{r},\vec{r}')\}} \sum_{\{n(\vec{r})\}} \exp\Bigg(\sum_{\langle r, r'\rangle} V_0(\theta(r) - \theta(r') - 2\pi m(r,r')) + \sum_{\vec{R}} (\ln y_0) f_0(S_{\vec{R}}(m)) + \sum_{\vec{r}} (\ln y_p) f_p(n(\vec{r})) + \sum_{\vec{r}} i n(\vec{r}) \theta(\vec{r}) p \Bigg). \tag{D19}$$

This is a very general form of the action. For the case of interest to us here,

$$V_0(\theta) = -\tfrac{1}{2} K \theta^2, \quad f_0(x) = f_p(x) = x^2. \tag{D20}$$

We have, in fact, calculated the dual of each and every term in Eq. (D19). Instead of recalculating, we simply present the result. After the dual transformation Eq. (D19) reads

$$Z(2\pi K, y_0, y_p) = \left(\prod_{\vec{R}} \int_0^{p} d\tilde{\phi}(\vec{R})\right) \sum_{\{\tilde{n}(\vec{R},\vec{R}')\}} \sum_{\tilde{m}(\vec{R})} \exp\Bigg(\sum_{\langle R, R'\rangle} \tilde{V}(\tilde{\phi}(\vec{R}) - \tilde{\phi}(R') - p\tilde{n}(R,R')) + \sum_{\vec{R}} \ln y_0 f_0(\tilde{m}(\vec{R})) + \sum_{\vec{r}} (\ln y_p) f_p(S_r(\tilde{n})) + \sum_{\vec{R}} 2\pi i \tilde{m}(R) \tilde{\phi}(R) \Bigg). \tag{D21}$$

The $\tilde{\phi}$ integrals can, if one desires, be extended to infinity by making suitable gauge transforms of the form

$$\tilde{\phi}(R) \to \tilde{\phi}(R) + p\tilde{n}(R), \qquad \tilde{n}(R,R') \to \tilde{n}(\tilde{R},\tilde{R}') + \tilde{n}(R) - \tilde{n}(R'). \tag{D22}$$

But, Eq. (D21) is quite sufficient for our purposes. If one uses the Villain form for V_0, i.e., that in Eq. (D20), then

$$\tilde{V}(\tilde{\phi}) = -(1/2K)\phi^2 - \tfrac{1}{2}\ln(2\pi K).$$

The difference in form between (D19) and (D21) will completely disappear if one defines a new integration variable in (D21), namely

$$\tilde{\theta}(R) = (2\pi/p)\phi(R).$$

In this way, we conclude that

$$Z(2\pi K, y_0, y_p) = Z(p^2/2\pi K, y_p, y_0)(p/2\pi K)^N, \tag{D23}$$

with N being the number of sites. Equation (D23) is the duality result which we sought.

Note added in proof. A superfluid layer provides a possible experimental realization of the pure planar model [see Doniach (Phys. Rev. Lett. 31, 1450 (1973)], and also private communications in which he kindly points out this omission in our thinking [an early theoretical calculation can be found in W. Kane and L. P. Kadanoff, Phys. Rev. 155, 80 (1967)]. See also the experiments by Reppy (to be published). In magnetic systems see the experiments by Y. S. Karimov and Y. N. Novikov [Zh. Eksp. Teor. Fiz. Pis'ma Red. 19, 268 (1974) Sov. Phys.-JETP Lett. 19, 159 (1974)]. We wish to thank V. Pokrovsky for pointing out this last reference to us.

The reader may want to compare the results of this Migdal style recursion calculation with that of Lublin [Phys. Rev. Lett. 34, 568 (1975)], who obtains a single nontrivial fixed point. Both calculations have similar defects in that they do not handle vortex pairs in an accurate fashion.

*Supported in part by NSF under Grant Nos. DMR 73-04886 A02 and MRL-NSF P-401 by Brown University Materials Research Laboratory.

†On leave from "Facultad de Ciencias," Universidad Nacional de Mexico.

‡Permanent address.

§ Work supported by a Junior Fellowship of the Harvard Society. Supported in part by NSF Grant No. DMR 72-02977 A03.

[1]H. E. Stanley and T. A. Kaplan, Phys. Rev. Lett. 17, 913 (1966).

[2]H. E. Stanley, Phys. Rev. Lett. 20, 589 (1968).

[3]M. A. Moore, Phys. Rev. Lett. 23, 861 (1969).

[4]N. D. Mermin and H. Wagner, Phys. Rev. Lett. 17, 1133 (1966).

[5]P. C. Hohenberg, Phys. Rev. 158, 383 (1967).

[6]D. Jasnow and M. E. Fisher, Phys. Rev. Lett. 23, 286 (1969).
[7]F. J. Wegner, Z. Phys. 206, 465 (1967).
[8]V. L. Berezinskii, Zh. Eksp. Teor. Fiz. 59, 907 (197x) [Sov. Phys.-JETP 32, 493 (1971)].
[9]J. Zittartz, Z. Phys. 23B, 55 (1976); 23B, 63 (1976).
[10]J. M. Kosterlitz and D. J. Thouless, J. Phys. C 6, 1181 (1973).
[11]V. L. Berezinskii, Zh. Eksp. Teor. Fiz. 61, 1144 (1971) [Sov. Phys.-JETP 34, 610 (1971)].
[12]J. M. Kosterlitz, J. Phys. C 7, 1046 (1974). Kosterlitz refers to the model considered here as the "two-dimensional classical xy model."
[13]A. Luther and D. J. Scalapino [Phys. Rev. B 16, 1153 (1977)] have produced solution of a planar Heisenberg model which is at least in rough accord with this spin-wave-vortex picture. See, however, the discussion in Sec. V.
[14]A. A. Migdal, Zh. Eksp. Teor. Fiz. 69, 1457 (1975).
[15]A. M. Polyakov, Phys. Lett. B59, 79 (1975).
[16]E. Brezin and J. Zinn-Justin, (a) Phys. Rev. Lett. 36, 691 (1976); (b) Phys. Rev. B 14, 3110 (1976).
[17]J. Villain, J. Phys. (Paris) 36, 581 (1975).
[18]Several investigators have made use of this mapping of the planar model onto an integer problem, including J. Villain [J. M. Kosterlitz (private communication)] and R. J. Meyerson (private communication).
[19]K. G. Wilson, Cargese 1976 Summer School Notes (unpublished); see also Ref. 14 of Ref. 16b.
[20]R. J. Birgeneau, H. J. Guggenheim, and G. Shirane, Phys. Rev. Lett. 22, 720 (1969); Phys. Rev. B 1, 2211 (1970).
[21]For a review, see L. J. Jongh and A. R. Miedema, Adv. Phys. 23, 1 (1974).
[22]V. L. Pokrovsky and G. V. Uimin, Phys. Lett. A45, 467 (1973); Sov. Phys.-JETP 38, 847 (1974).
[23]J. M. Kosterlitz and D. J. Thouless, Prog. Low Temp. Phys. (to be published).
[24]E. Domany (private communication) has pointed out to us that the leading symmetry-breaking term which can enter (1.1) in an *antiferromagnet* with a local p-fold symmetry is proportional to $\cos^2 p\theta$ for p odd. Thus, the effective p which enters in this case is $p_{\text{eff}} = 2p$.
[25]L. P. Kadanoff, Ann. Phys. (N.Y.) 100, 359 (1976).
[26]D. R. Nelson and M. E. Fisher, Ann. Phys. (N.Y.) 91, 226 (1975).
[27]The case $p = 4$ has been discussed recently by A. Aharony, Symposium on Renormalization Group in Physics, Trondheim (Norway), 1976 (unpublished).
[28]A. A. Migdal [D. J. Wallace (private communication)] has also considered approaching the planar model in this way.
[29]The dual (4.2) of the Villain model is identical with a model proposed by S.-T. Chui and J. D. Weeks [Phys. Rev. B 14, 4978 (1976)] to describe the spontaneous growth of steps on a crystalline interface in contact with solution.
[30]See F. Spitzer, *Principles of Random Walk* (Van Nostrand, Princeton, 1964), pp. 148–151.
[31]See, e.g., M. E. Fisher, *Lectures in Theoretical Physics* (University of Colorado, Boulder, Colo.), Vol. VIIC.
[32]Kosterlitz used a slightly different definition of y, and his coupling J is one half of ours.
[33]High-temperature series expansions supporting the exponential behavior of the correlation length above T_c have been found by W. J. Camp and J. V. Van Dyke, J. Phys. C 8, 336 (1975).
[34]In a separate communication [J. José, Phys. Rev. D 14, 2826 (1976)] it was found that the Green's function (in the continuum limit) for the sine-Gordon field theory in (1+1) dimensions as calculated by S. Coleman [Phys. Rev. D 11, 2088 (1975)] is the same as that given in Eq. (1.3). This in turn suggested the correspondence vortex -- soliton at low temperatures. Luther pointed out (private communication) the apparent inconsistency of the connection of the planar model (in the absence of symmetry breaking fields) with a massive theory. From the discussion in Sec. IV we can see how the effect of the vortex excitations reconciles this problem.
[35]This is consistent with the recent molecular-dynamics results of T. Schneider and E. Stoll, Phys. Rev. Lett. 36, 1501 (1976).
[36]R. A. Pelcovitz and D. R. Nelson, Phys. Lett. A57, 23 (1976); E. Brezin, J. Zinn-Justin, and J. C. LeGuillou, Phys. Rev. B 14, 4976 (1976).
[37]Correction of this type, which cannot be seen in standard perturbation theory in K^{-1}, plus the topology of the order parameter are, in a sense, responsible for the critical properties of the planar model.
[38]This approach has also been employed by E. K. Riedel (private communication).
[39]See, e.g., L. P. Kadanoff, in *Proceedings of the Enrico Fermi Summer School of Physics, Varenna, 1970,* edited by M. S. Green (Academic, New York, 1971).
[40]L. P. Kadanoff, Rev. Mod. Phys. 49, 267 (1977).